Antimicrobial activity and mechanism of antimicrobial peptide Hylin a1 and its analog peptides against multidrug resistant bacteria

항생 펩타이드 Hylin a1 과 그 유사체 펩타이드의 항균 활성 및 작용기작에 관한 연구

February 25, 2020

Graduate School of Chosun University

Department of Life Science

Hee Joo Park

Antimicrobial activity and mechanism of antimicrobial peptide Hylin a1 and its analog peptides against multidrug resistant bacteria

Advisor : Prof. Yoonkyung Park

A thesis submitted to the Graduate School of the Chosun University in partial fulfillment of the requirements for the Master of Science

October 2019

Graduate School of Chosun University

Department of Life Science

Hee Joo Park

February 2020

Thesis for Master Degree

Antimicrobial activity and mechanism of antimicrobial peptide Hylin a1 and its analog peptides against multidrug resistant bacteria

Graduate School of Chosun University

Departmemt of Life Science

Hee Joo Park

Hee Joo Park's master thesis
has approved by

Chairman Hongsung Chun

Committee Members Seok-Jun Kim

Yoonkyung Park

November 2019

Graduate School of Chosun University

CONTENTS

LIST OF TABLES

LIST OF FIGURES

LIST OF ABBREVIATIONS

AMP	Antimicrobial peptide
Fmoc	9-fluorenylmethoxycarbonyl
HBTU	2-(1H-benzitruazole-1-yil)-1,1,3,3-tetramethyluronium
DMF	Dimethylformamide
HOBt	*N*-hydroxybenzotriazole
DIEA	*N*,*N*-diisopropylethylamine
NMP	*N*-methylpyrrolidone
DCM	Dichloromethane
TFA	Trifluoroacetic acid
SDS	Sodium dodecyl sulfate
TFE	Trifluoroethanol
CD	Circular dichroism
MHB	Mueller Hinton broth
MIC	Minimal inhibitory concentration
CV	Crystal violet
PE	Phosphatidylethanolamine
PG	Polyethylene glycol
CH	Cholesterol
PC	Phosphatidylcholine

NPN	*N*-phenyl-a-naphthylamine
ONPG	*ortho*-nitrophenyl-β-galactoside
$diSC_3$-5	3,3'-dipropylthiadicarbocyanine iodide
PI	Propidium iodide
LPS	Lipopolysaccharide
LTA	Lipoteichoic acid
DMEM	Dulbecco's modified Eagle's medium
FBS	Fetal bovine serum

초 록

항생 펩타이드 Hylin a1 과 그 유사체 펩타이드의 항균 활성 및 작용기작에 관한 연구

박 희 주

지 도 교 수 : 박 윤 경 Ph D.

조 선 대 학 교 대 학 원

생 명 과 학 과

항생제 오남용 문제로 인한 항생제 내성은 점점 가속화되고 있다. 스스로를 방어하기 위해 만들어낸 자체 방어 능력을 지닌 다제 내성 균주가 증가함으로써 심각한 결과가 초래되고 있다. 항생제의 개발에도 불구하고, 이용 가능한 약제의 수가 제한되어 치료가 불가능한 상황이다. 이로 인해, 항생제를 대체할 수 있는 후보 물질로 항균 펩타이드(antimicrobial peptide, AMP)가 주목받고 있으며, 그에 대한 개발은 점차 증가하고 있다. AMP 는 대부분 유기체에서 발견되며, 구조적으로 10-50 개의 아미노산으로 이루어져 있고 주로 양전하를 띠며 30% 이상의 소수성 아미노산 잔기를 포함하고 있다. 이러한 특징으로 인해 음전하를 가지는 박테리아의 막과 접촉하게 되면 세포막을 파괴시키거나 구멍을 내고 세포막의 전위를 소실시켜 박테리아의 사멸을 유도하기도 한다. 이러한 항생 펩타이드는 다양한 항균 작용 기작을 가지고 있으며 구조적, 기능적 다양성을 나타낸다. 이전의

연구에서, 전기 자극을 받은 남미 개구리의 점액질에서 분리된 Hylin a1 은 그람 음성 및 그람 양성 균주에 대해 항 항균 활성을 보이지만 적혈구 세포에 강한 용혈 현상을 보이는 18 개의 아미노산으로 확인되었다. 본 연구에서는, Hylin a1 의 잔기를 바탕으로 페닐 알라닌을 알라닌으로 치환한 Hylin a1-2A 와 글라이신을 라이신으로 치환한 Hylin a1-3K, Hylin a1-11K 와 Hylin a1-15K, 총 4 개의 유사체 펩타이드를 디자인하였다. 이러한 유사체 펩타이드는 Hylin a1 보다 그람 음성, 그람 양성 및 내성 균주에 뛰어난 항균 효과를 보였으며, 바이오필름 억제와 제거 효과가 매우 우수함을 확인하였다. Hemolysis assay 를 통해 Hylin a1 에서 보였던 용혈 현상이 유사체 펩타이드에서는 현저히 줄어드는 결과를 관찰하였다. 그람 음성 및 그람 양성 박테리아의 대표 균주를 선정하여 유사체 펩타이드에 의한 박테리아 사멸 속도를 확인하였으며, Hylin a1-11K 및 Hylin a1-15K 가 10 분 이내에서 가장 빠르고 효과적으로 작용한다는 것을 확인하였다. 또한 생체 내의 안정성을 확인하기 위해 여러가지 염 농도와 사람의 혈청에서 항생 펩타이드의 항 미생물 효과를 확인하였으며, 그 결과 Hylin a1-11K 및 Hylin a1-15K 가 생체 내의 조건에서도 안정성을 가지며, 효과적으로 박테리아를 억제할 수 있다는 결과를 확인하였다. 또한, 원편광 이색성 분광법 (Circular dichroism, CD) 을 이용하여 박테리아 막의 유사 환경에서 유사체 펩타이드의 이차 구조 분석을 분석한 결과, 결합 친화성을 가지는 알파 헬릭스 구조를 가지는 것으로 확인하였다. 이러한 생물학적 활성 분석을 바탕으로 유사체 펩타이드의 작용기전을 살펴보기 위해, 독소 인자인 LPS 와 LTA 에 대한 결합 친화성을 CD spectroscopy 를 측정하였다. 그 결과, Hylin a1-11K 와 Hylin a1-15K 는 모두 결합 친화성을 가졌으며, Hylin a1-2A 와 Hylin a1-3K 는 선택적으로 LTA 에서만 친화성을 가졌다. 또한 인공적인 리포좀을 형성하여 형광물질인 calcein 의 방출을 측정함으로써 포유류와 유사한 구성의 lipid 와 박테리아 유사 lipid 에서 선택성을 가진다는 것을 확인하였다. n-phenyl-1-

naphthylamine (NPN)를 이용한 외막 투과성 분석과 ortho-nitrophenyl-β-galactoside (ONPG) 을 이용한 내막 투과성 분석, 3,3′-dipropylthiadicarbocyanine iodide ($diSC_3$-5) 을 이용한 전위차에 따른 막 투과성 분석, SYTOX green 과 Propidium iodide (PI) 을 이용한 원형질막 투과성 분석 실험을 통해 유사체 펩타이드는 완전히 박테리아 막을 표적으로 작용하는 메커니즘을 규명하였다. 유사체 펩타이드 Hylin a1-11K 와 Hylin a1-15K 는 마우스의 마크로파지 세포에서 TNF-α, IL-6, IL-1β 와 같은 염증인자의 발현이 현저히 줄어든다는 결과를 확인하였으며, 결과적으로 유사체 펩타이드는 뛰어난 항 미생물 활성을 가졌으며, 독성 또한 현저히 줄어들었다. 항 바이오필름 효과와 박테리아 막을 완전히 분열시킨다는 메커니즘을 입증하였으며, 항 염증반응 효과를 확인하였다. 결과적으로, Hylin a1 을 바탕으로 몇 개의 잔기를 치환한 유사체 펩타이드는 항 미생물 효과와 항 바이오필름 활성 및 항 염증 효과가 있음을 증명하였으며, 항생제를 대체할 만한 antimicrobial peptide 로써 활용가치가 있다고 전망된다.

Abstract

Antimicrobial activity and mechanism of antimicrobial peptide Hylin a1 and its analog peptides against multidrug resistant bacteria

Hee Joo Park

Advisor : Prof. Yoonkyung Park, Ph. D.

Department of Life Science

Graduate School of Chosun University

The increase in the prevalence of multidrug-resistant bacterial strains due to the misuse of antibiotics has serious consequences on human health. Despite the development of antibiotics, in some situations, treatment is limited by the small number of antibiotics currently available. Antimicrobial peptides have attracted attention as new drug candidates and their development is progressing. In a previous study, Hylin a1, isolated from the skin of electrically stimulated Latin American frogs, showed antimicrobial activity against Gram-negative and Gram-positive bacteria; Hylin a1 was identified as an 18-amino acid antimicrobial peptide with strong hemolytic activity against red blood cells. In this study, Hylin a1-2A, Hylin a1-3K, Hylin a1-11K, and Hylin a1-15K were formed by substituting lysine (K) and alanine (A) based on the residues of Hylin a1. The analog peptides showed better antimicrobial effects against Gram-negative bacteria, Gram-positive bacteria, and resistant strains than Hylin a1 and effectively inhibited and reduced biofilm formation. Hemolysis analysis showed that analog peptides are less toxic to red blood cells than Hylin a1. Hylin a1-11K and Hylin a1-15K appeared quickly and efficiently within 10 min according to measurements of the rate of action of the peptide toward bacteria. In addition, at

various salt concentrations and in the presence of human serum, Hylin a1-11K and Hylin a1-15K effectively inhibited bacteria. Secondary structure analysis of analog peptides in membrane-like environments by circular dichroism spectroscopy revealed α-helix structures. Based on the biological activity assay, circular dichroism spectroscopy was performed to measure the binding affinity for Gram-negative and Gram-positive bacteria, lipopolysaccharide, and lipoteichoic acid. Consequently, Hylin a1-11K and Hylin a1-15K showed binding affinity, whereas Hylin a1-2A and Hylin a1-3K exhibited selective affinity only in lipoteichoic acid. In addition, liposome formation and measurement of the release of fluorescent calcein confirmed the selectivity in lipids such as bacterial and mammalian cell membranes. N-phenyl-a-naphthylamine, ortho-nitrophenyl-β-galactoside, 3,3'-dipropylthiadicarbocyanine iodide, and SYTOX green uptake and propidium iodide revealed that the analog peptides completely disrupted the bacterial membrane. Hylin a1-11K and Hylin a1-15K significantly reduced the expression of pro-inflammatory cytokines in mouse macrophage cells. Hylin a1-11K and Hylin a1-15K exhibited significant therapeutic effects upon infection with the multidrug-resistant strain of Acinetobacter baumannii. Overall, analog peptides in which several residues were substituted based on Hylin a1, showed antimicrobial and anti-inflammatory effects and may serve as the next-generation antimicrobial peptides that can replace antibiotics.

I. Introduction

Agents that can respond to rapidly emerging antibiotic-resistant bacterial strains are urgently needed. Currently, a group of bacteria, known as ESKAPE, is having a major impact on society[1], because of their resistance to antibiotics. ESKAPE comprises the following species: *Enterococcus spp.*, *Staphylococcus aureus* (*S. aureus*), *Klebsiella pneumoniae* (*K. pneumoniae*), *Acinetobacter baumannii* (*A. baumannii*), *Pseudomonas aeruginosa* (*P. aeruginosa*), *Enterobacter spp*., and *Staphylococcus aureus* (*S. aureus*), which commonly cause community infection [2]. Particularly, *A. baumannii* is a high-risk antibiotic-resistant bacterium, as designated by the World Health Organization [3], and the proportion of strains resistant to various antibiotics, including carbapenems (imipenem and meropenem), is increasing. This is because many multidrug-resistant bacteria are resistant to several antibiotics simultaneously [4].

Antimicrobial peptides (AMPs) have gained attention as alternatives for preventing this resistance [5]. AMPs may be useful as new therapeutics for multidrug-resistant bacteria, and thus studies are being conducted to develop antimicrobial peptides [6]. AMPs are important components of innate immunity and are found in organisms such as plants, animals, marine organisms, Insects, and have direct antimicrobial activity and immunomodulatory properties [7-9]. In addition, AMPs selectively act on target cells and do not induce an immune response because they are not digested and accumulated by enzymes in the body and are recognized and self-cleaved to form amino acids. AMPs consist of 10–50 amino acids, mainly with a positive charge (+2–+9), and contain more than 30% hydrophobic amino acid residues [10]. Thus, when AMPs contact a negatively charged bacterial cell membrane, an amphipathic alpha-helix structure is formed, and this directly destroys or punctures the cell membrane to lose its potential. Recently, AMPs have been reported to penetrate cell membranes and act on intracellular targets rather than acting directly on bacterial cell membranes and use varying mechanisms [8, 11]. However, AMPs

have short half-lives, high toxicity, and protease cleavage. Recently, AMPs have been studied under *in vivo* conditions to compensate for these weaknesses.

In a previous study, Hylin a1 was isolated from the arboreal South American frog *Hypsiboas albopunctatus* and contains 18 amino acid residues. It is active against Gram-negative and Gram-positive bacteria. However, at 18 μM it is toxic to human red blood cells (RBCs) [12].

In this study, we designed 18 amino acid analog peptides for Hylin a1. We generated peptides with strong antimicrobial activity and low toxicity by replacing the second and third of parent peptide (Hylin a1) to alanine (A) and lysine (K). The activity of Gram-negative bacteria, Gram-positive bacteria, and resistant strains on *A. baumannii* and *S. aureus* and their toxicity toward erythrocytes were investigated. The mechanism of action of the synthesized peptides on bacteria was studied. Among them, Hylin a1-11K and Hylin a1-15K were studied for their antimicrobial, anti-biofilm, and anti-inflammatory activities. The purpose of this study was to develop analog peptides with lower hemolytic action and more potent activity than the parent peptide Hylin a1, as well as to confirm the possibility of using Hylin a1 as a therapeutic agent for overcoming multidrug resistant strains (MDR).

Ⅱ. Materials and Methods

1. Materials

1.1 Materials

L-α-phosphatidylglycerol (PG, from *E. coli*), 1-α-phosphatidylethanolamine (PE), 1-α-phosphatidylcholine (PC, from egg yolk), cholesterol (CH, from porcine liver) and Sodium dodecyl sulfate (SDS), Trifluoroethanol (TFE), *ortho*-nitrophenyl-β-galactoside (ONPG), n-phenyl-1-naphthylamine (NPN), Propidium iodide (PI), 3,3'-dipropylthiadicarbocyanine iodide ($diSC_3$-5) were obtained from Sigma-Aldrich (St Louis, MO, USA). Dulbecco's Modified Eagle's Medium (DMEM) were obtained from Welgene (South Korea) and Fetal bovine serum (FBS) were obtained from Gibco (Grand island, NY, USA).

1.2 Microbial strains

E. coli ATCC 25922, *P. aeruginosa* ATCC 27853 and *S. aureus* ATCC 25923 were obtained from ATCC (American Type Culture Collection; Masassas, VA, USA). *A. baumannii* KCTC 2508, *B. cereus* KCTC 1012, *S. typhimurium* KCTC 1926 were obtained from KCTC (Korean Collection for Type Cultures, KRIBB, Daejeon, South Korea). MDR bacteria (Strains of EJ *S. aureus* 1 - 13 and EJ *A. baumannii* 1 - 26) isolated from patients were obtained from EULJI university hospital (Daejeon Medical Center, EULJI University).

2. Methods

2.1 Peptides

2.1.1. Peptide Design and Sequence Analysis

The peptides were designed by truncating and substituting residues based on the helical wheel diagram and tree-dimensional structure of Hylin a1 to design the analog peptides Hylin a1-2A, Hylin a1-3K, Hylin a1-11K, and Hylin a1-15K based on a helical wheel projection and its three-dimensional structure. The helical wheel projection was performed online using HeliQuest (http://heliquest,ipmc,cnrs,fr). Amino acid sequence analysis of peptides was performed online using the Mobyle@RPBS bioinformatics portal (http://mobyle.rpbs.univ-paris-diderot.fr/cgi-bin/portal.py#welcome).

2.1.2. Peptide Synthesis and Purification

The peptides were synthesized with the solid-phas-9-fluorenylmethoxycarbonyl (Fmoc) method as reported previously [13] on a Rink amide 4-methylbanshydrylamine resin using a Liberty microwave peptide synthesizer (CEM, Matthews, NY, USA). The following chemicals were used as linkage reagents: 0.45 M 2-(1H-baczotriazole-1-yil)-1,1,3,3-tetramethyluronium hexafluorophosphate diluted in dimethylformamide, 0.1 M *N*-hydroxybaczotriazole diluted in piperidine/dimethylformamide, and 2 M *n*,*n*-diisopropylethylamine diluted in *n*-methylpyrrolidone. After washing with dichloromethane, cleavage was performed by incubation for 2 h at 25°C in a trifluoroacetic acid solution containing water, phenol, and triisopropylsilane. The crude peptide was precipitated by dilution with ice-cold diethyl ether, and then spread on the tube wall and dried. After resuspension in 25°C water, the peptide was purified by reversed-phase high-performance liquid chromatography on a Jupiter C18 column (4.6 × 250 mm, 300 Å, 5 μM; Phenomenex, Torrance, CA, USA). The molecular weights of the synthetic peptides were confirmed by matrix-assisted laser desorption ionization-time of flight (MALDI-TOF) mass spectrometry. The peptides were dissolved in deionized water and solutions were stored at -20°C.

All peptides used were > 95% pure.

2.1.3. Mass Spectrometry

The molecular weight of synthetic peptides was determined by MALDI-TOF mass spectrometry (Kratos Analytical, Inc., Chestnut Ridge, NY, USA).

2.2 Activity tests

2.2.1. Antibacterial Activity Assay

We detected the antimicrobial activity of the peptide against Gram-negative, Gram-positive, and MDR bacteria. The minimal inhibition concentrations (MICs) of parent and analog peptides were determined using the microbroth dilution method [14]. Bacterial strains were cultivated by shaking overnight at 37°C in Mueller-Hinton broth (MHB). On the next day, the culture was diluted to 2×10^5 CFU/mL in MHB medium. The peptides were serially diluted concentrations ranging from 0.5 to 32 μM in 10 mM sodium phosphate buffer, and then added to a 96-well plate. In each well, 50 μL bacterial aliquots were mixed with an equal volume of peptide solution, and incubated at 37°C for 18 h. Inhibition of bacterial growth was determined by measuring the absorbance at 600 nm using a Versa Max microplate reader (Molecular Devices, Sunnyvale, CA, USA). The MIC of each peptide was defined as the lowest peptide concentration at which no bacterial growth was observed. The test was performed in triplicate.

2.2.2. Hemolysis Assay

To confirm hemolysis of sheep RBCs (sRBCs) against peptides, fresh sheep blood samples

were centrifuged at 2000 ×g for 10 min at 4°C and washed three times with phosphate-buffered saline (PBS). The sRBCs were diluted with PBS to a final concentration of 8%. Peptides were serially diluted from 0 to 50 μM, and the sRBS suspension was added to 96-well plates (100 μL/well) and reacted in a gently shaking incubator at 30 ×g for 1 h at 37°C. The plate was centrifuged 1500 ×g for 10 min, and 100 μL of the supernatant was transferred to a new 96-well plate. The absorbance at 414 nm was measured with a Versa-Max ELISA reader (Molecular Devices). sRBCs treated PBS were used as the negative control, whereas cells treated with 0.1% Triton X-100 was used as a positive control. The hemolysis rate induced by each peptide in erythrocytes was calculated using the following equation:

$$\% \text{ Hemolysis} = [(Abs_{414nm} \text{ in the peptide solution} - Abs_{414nm} \text{ in PBS}) /$$

$$(Abs_{414nm} \text{ in 0.1\% Triton X-100} - Abs_{414nm} \text{ in PBS})] \times 100$$

2.2.3. Time Killing Assay

A time-kinetic analysis was performed to analyze the time zone effects of peptides on in vitro bacteria against microbial populations. *A. baumannii* KCTC 2508 and *S. aureus* ATCC 25923 were cultured overnight, and cell density was measured (2×10^5 CFU/mL) in MHB medium. The peptides were diluted to final concentrations of 1x, 2x, or 4x MIC, respectively. Cells and peptides were reacted by mixing 50 μL of the same amount and spread in MHB agar medium at different times (0, 5, 10, 15, 20, 25, 30, 45, 60, 90, 120 min). Additionally, the cells were incubated for 24 h and the number of colonies was counted on the next day. All experiments were performed in triplicate.

2.2.4. Anti-biofilm Inhibition Assay

To compare the ability of the bacterial strains to form biofilms in the absence and presence of the peptides, standard strains of *A. baumannii* KCTC 2508, *S. aureus* ATCC 25923, and clinical isolated MDR strains (EJ *A. baumannii* 1–26, EJ *S. aureus* 1–13) were cultured in MHB media at 37°C incubation. Bacterial suspensions (5×10^5 CFU/mL) in MHB media supplemented with 0.2% glucose were added to a 96-well plate (50 μL/well). Next, 50 μL of each serially diluted peptide (0–32 μM) was added to the 96-well plate and incubated 24 h at 37°C. After incubation, 100 μL of the culture supernatant was discarded. The biofilms were fixed with 100 μL of 100% methanol for 15 min, and then air-dried. The biofilms were stained with 0.1% crystal violet [15] for 30 min and rinsed three times with distilled water. After adding 200 μL of 95% ethanol, the biofilm mass was quantified by measuring the OD at 595 nm using a Versa-Max microplate ELISA reader. The results were calculated as the percentage of biofilm formed with respect to the control. All experiments were performed in triplicate.

2.2.5. Anti-biofilm Reduction Assay

To confirm that the peptide effectively removed the biofilm, the peptide was treated for 24 h after the biofilm was formed. The standard strains *A. baumannii* KCTC 2508, *S. aureus* ATCC 25923, MDR strains EJ *A. baumannii* 10, 24, and EJ *S. aureus* 5, 11, were incubated in 90 μL of 5×10^5 (CFU/mL) MHB media with 0.2% glucose in a 96-well plate and then at 37°C for 24 h. On the next day, each peptide was serially diluted to 0, 2, 4, 8, 16, 32, 64, or 128 μM in full MHB medium, treated with 10 μL of diluted peptide, and reacted for 24 h.

Control wells contains only MHB medium. To quantify biofilm formation, the supernatant were discarded from each well, and then 100 μL of 100% methanol was added and incubated for 15 min followed by staining with 100 μL of 0.1% crystal violet for 30 min. Excess stain was rinsed off three times with deionized water, and 200 μL of 95% ethanol was added and the biofilm mass

was quantified based on the OD_{595} using a Versa-max microplates ELISA reader. The results were calculated as the percentage of biofilm formed with respect to the controls.

2.2.6. Visualization of Biofilms

To visualize the ability of the peptide to remove the biofilm, 100 μL of aliquots of *A. baumannii* and *S. aureus* strains were cultured in MHB. Bacteria were diluted to 5×10^5 CFU/mL in 0.2% glucose contained MHB media at 37°C for 24 h. On the next day, the culture medium was discarded and the serially diluted peptides were added at up to 128 μM in MHB containing 0.2% glucose for 24 h. The culture medium were discarded, and wells were carefully washed with PBS to remove planktonic bacteria. The biofilms were fixed with 100% methanol for 15 min and stained with SYTO9 dye for 30 min in the dark. Images were obtained using an EVOS FL Auto 2 Fluorescence microscope (Invitrogen, Carlsbad, CA, USA).

2.2.7. Salt Stability Assay

Salt stability was analyzed by treating various salts in the presence the peptides. The standard strains *A. baumannii* KCTC 2508 and *S. aureus* ATCC 25923 were cultured in MHB media at 37°C for 17–18 h. Bacteria strains were diluted to 2×10^5 CFU/mL in MHB media. The peptides were serially diluted from 0 to 32 μM in the presence of physiological salts. The final concentrations of physiological salts were 50, 100, and 150 mM NaCl, 0.5, 1, and 2 mM $MgCl_2$, and 2, 4, and 8 μM $FeCl_3$. The procedure was the same as that used in the MIC assay.

2.2.8. Serum Stability Assay

We confirmed the stability of human serum with analog peptides in the presence of bacteria at 5% and 10% human serum (Sigma-Aldrich). The serum stability test was conducted using the MIC method. Bacteria were cultured in MHB media at 37°C overnight. On the next day, the bacteria density was measured (2 × 105 CFU/mL). Human serum was diluted in MHB media at 5% and 10% and then peptides were serially diluted from 0 to 64 μM in MHB media diluted with human serum. The bacteria resuspension was added to a 96-well plate. After 17–18 h, stability was determined by measuring the absorbance at 600 nm using a Versa Max microplate reader. The test was performed in triplicate.

2.3 Mechanism of Action

2.3.1. Circular Dichroism Measurements

Circular dichroism (CD) spectrum analysis was performed to estimate the secondary structure of the peptides in a membrane mimic environment with various solutions. Both peptides were dissolved in solutions containing 10 mM sodium phosphate buffer (mimicking an aqueous environment), 30 mM sodium dodecyl sulfate (mimicking the anionic environment of bacterial membranes), and 50% 2,2,2-trifluoroethanol (mimicking the hydrophobic environment of the microbial membrane). Peptides concentration were fixed to 40 μM. CD spectra were measured using a JASCO 810 spectropolarimeter (Jasco, Tokyo, Japan), with a 0.1-cm quartz cuvette at 25°C. CD spectra were recorded from 190 to 250 nm.

2.3.2. Preparation of lipids and Calcein Leakage Assay

Vesicle preparations were used for freeze-thaw method [15, 16], The following lipid mixtures were prepared: egg phosphatidylcholine (egg PC) and cholesterol (CH) at a 10:1 (w/w) and

phosphatidylethanolamine (PE) and polyethylene glycol (PG) at a 7:3 (w/w). The preparation was mixed with chloroform, and then argon gas was used to remove the chloroform after mixing the vesicles. The remaining chloroform was removed by 1–2 h of lyophilization. On the next day, the dry lipid films were resuspended in a dye buffer solution (70 mM Calcein in PBS, pH7.3), followed by freezing of the lipid suspension in liquid nitrogen and thawing in a 50°C water bath; the freeze-thaw cycle was repeated more than 15 times. The lipid suspension was extruded through a 0.4-μM pore polycarbonate membrane. A gel chromatography Sephadex G-50 column was used to separate the free calcein, and calcein entrapped lipids were diluted to at the diversity ratio. Calcein leakage were measured using a Spectramax M3 spectrophotometer (Molecular Devices) at an excitation of 480 nm and emission of 520 nm. PBS was used as a negative control, and 0.1% Triton X-100 was used as a positive control with calcein-entrapped lipid. The percentage of dye leakage was calculated as follows:

$$\text{Percentage of dye leakage} = \frac{F - F_0}{F_t - F_0} \times 100\%$$

2.3.3. Visualization of Liposome leakage

Calcein leakage visualization were examined by acquiring fluorescent images of the wells; 90 μL of prepared LUVs and 10 μL of peptides diluted in PBS were added to the 96-well black plates at various ratios and reacted for 30 min. Images were obtained using a Fluorescence-labeled organism bioimaging instrument (FOBI; Neo Science, Daejeon, Korea).

2.3.4. Outer Membrane Permeabilization Assay

The assay was confirmed by evaluating NPN uptake to determine the permeabilization activity

of the outer membrane of the peptide [17]. *A. baumannii* KCTC 2508 and *S. aureus* ATCC 25923 were grown to mid-log phase in MHB at 37°C, and both cultures were harvested by centrifugation in 5 mM HEPES buffer (pH 7.2) at 3000 ×g for 10 min and washed three times. Next, 100 μL of the cell suspension (OD_{600} = 0.25) was mixed with 50 μL of 10 μM NPN (dissolved in 95% ethanol) in 96-well black plates. Background fluorescence was measured at an excitation of 350 nm and emission of 420 nm and then different concentrations of peptides (0.5x, 1x, 2x, or 4x MIC) or 0.1% Triton X-100 (positive control) were added. NPN fluorescence was analyzed at an excitation of 350 nm and emission of 420 nm for 5–30 min using a micro-plate reader.

2.3.5. Cytoplasmic Membrane Depolarization Assay

The membrane depolarization activity of the peptides was determined using *A. baumannii* KCTC 2508 and *S. aureus* ATCC 25923 and membrane potential-sensitive fluorescence dye $dISC_3$-5. Bacteria were cultured in MHB at 37°C and harvested by centrifugation in 5 mM HEPES and 20 mM glucose (pH 7.3) at 3000 ×g for 10 min three times. After washing, the bacteria were resuspended to an OD_{600} of 0.05 in 5 mM HEPES, 20 mM glucose (pH 7.3), and 0.1 M KCL. dISC3-5 dye was added to the resuspended bacteria at a final concentration of 1 μM. After stabilization for 30 min at 37°C, 150 μL of the mixture was transferred into 96-well black plates. Background fluorescence was measured at an excitation of 622 nm and emission of 670 nm for 10 min. Next, 50 μL of peptides (0.5x, 1x, 2x, and 4x MIC) were added to the wells, and fluorescence was monitored at an excitation of 622 nm and emission of 670 nm for 1 h.

2.3.6. Inner Membrane Permeability Assay

The ability of the peptides to permeate the inner membrane of *E. coli* ATCC 25923 was assessed

using ONPG. This experiment was performed to evaluate the effect of the antimicrobial on the induction of β-galactosidase. Escherichia coli was cultured in LB media containing 0.2% lactose at 37°C, washed, and collected to a final density of OD_{600} = 0.2 in sodium phosphate buffer (pH 7.2). Next, 50 μL of peptides at the 0.5x, 1x, 2x, and 4x MIC were mixed with 50 μL of 6 mM ONPG in 96-well microplates. A control without *E. coli* was measured at A_{420} nm. Next, 100 μL of *E. coli* (OD_{600} = 0.2) was mixed. The time dependence of the relative fluorescence intensity was measured using a Versa-Max microplate reader at 420 nm.

2.3.7. SYTOX green Uptake Assay

A. baumannii KCTC 2508 and *S. aureus* ATCC 25923 were cultured overnight in MHB media and harvested by centrifugation at 4000 ×g for 10 min. The cells were washed with sodium phosphate buffer (pH 7.4) three times and then resuspended in SP buffer. The cell density was measured at an OD_{600} = 0.5. SYTOX green was added and the samples were incubated for 15 min in the dark at a final concentration of 1 μM. Background fluorescence was measured in the control at an excitation of 485 nm and emission of 520 nm for 10 min. The analog peptides diluted to their final concentrations (0.5 x, 1 x, 2 x, and 4 x MIC) were added, and fluorescence intensity was measured using a micro-plate reader at an excitation of 485 nm and emission of 520 nm for 1 h at 5-min intervals.

2.3.8. Flow Cytometry

To investigate bacterial membrane disruption by flow cytometry, *A. baumannii* KCTC 2508 and *S. aureus* ATCC 25923 were cultured in MHB media at 37°C, washed in PBS (pH7.2) 3 times, and resuspended. Cell density was measured at OD_{600} = 0.2 and 0.4, respectively. The cells were

treated with PI at a final concentration of 10 μg/mL and mixed with the peptides at 1x MIC, which was reacted for 10 min of incubation at 37°C. The samples were centrifuged at 10,000 ×*g* for 10 min and resuspended in 500 μL PBS. Analysis was performed using a CytoFLEX flow cytometer (Beckman Coulter, Brea, CA, USA).

2.4 Anti-Inflammation effect

2.4.1. Cell Culture and Infection

Raw264.7 (mouse macrophage cells) were cultured in DMEM containing 10% heat-inactivated FBS and 1% penicillin/streptomycin (WELGENE) at 37°C in a humidified atmosphere of 5% CO_2. The cells were seeded at a density 5×10^5 cell/wells in a 60-mm dish. After incubation overnight, EJAB 10 was washed in DPBS 3 times. Bacteria density was measured at 1×10^6 CFU/mL in DMEM containing 10% heat-inactivated FBS without antibiotics. Next, the medium from the 60-mm dish was discarded, and the wells were inoculated with 2 mL of EJAB 10 suspensions. After 1 h, Hylin a1-11K and Hylin a1-15K were added to the bacteria-inoculated dish at concentrations of 0.5x and 1 x MIC and incubation for 10 h at 37°C. After 10 h of incubation, the bacteria were removed and washed twice with cold DPBS.

2.4.2. Gene Expression Analysis for Real-time PCR (qPCR)

The effect of Hylin a1-11K and Hylin a1-15K on pro-inflammatory cytokine expression in EJAB 10 infected Raw264.7 cells was evaluated. Harvested Raw264.7 cells were isolated using TRIzol reagent (Life Technologies, Carlsbad, CA, USA), after which cDNA was synthesized using a TOPscript™ RT DryMIX cDNA synthesis kit (Enzynomics, Daejeon, South Korea). qRT-

PCR were performed with TOPreal qPCR 2x premix (SYBR green) using a 7500 real-time PCR system (Applied Biosystems, Foster City, CA, USA) and primers for the TNF-α, IL-6, and IL-1β genes. The amplification reaction was performed with 10 min denaturation at 95°C. The qPCR protocol was as follows: 40 cycles of 95°C for 15 s, 60°C for 30 s, and 72°C for 30 s. For mRNA quantification, expression levels were normalized to that of β-actin. Each sample was analyzed in triplicate. Primers sequences are shown in Table 7.

III. Results

1. Design and Characteristics of Synthetic Peptides

Hylin a1 was isolated from the electro-stimulated arboreal South American frog *Hypsiboas albopunctatus* [12]. The analog peptide was synthesized by substituting residues alanine and lysine. The synthesized peptide was synthesized by replacing the second residue with alanine and replacing the third with lysine. In addition, analog peptides were formed using the 11th and 15th lysine residues, respectively. The sequence of the peptides were IFGAILPLALGALKNLIK-NH_2 (Hylin a1), IAGAILPLALGALKNLIK-NH_2 (Hylin a1-2A), IAKAILPLALGALKNLIK- NH_2 (Hylin a1-3K), IAKAILPLALKALKNLIK- NH_2 (Hylin a1-11K) and IAKAILPLALKALKKLIK- NH_2 (Hylin a1-15K).

The observed and calculated molecular weight, hydrophobic moment, and retention time of each peptide are shown in Table 1. Molecular weight of Hylin a1-2A, Hylin a1-3K, Hylin a1-11K, and Hylin a1-15K were calculated as 0.393, 0.420, 0.471, and 0.482, respectively, and that of the parent peptide was 0.473. The net charge value of the analog peptide also increased from +2 to +5. All analog peptides except for Hylin a1-2A (+2) were more positively charged than Hylin a1 (+2). Spiral wheel diagrams and three-dimensional structural projections for the parent and analog peptides are shown in Figure 1. The molecular weights of Hylin a1 and its analog peptides were measured by MALDI-TOF/MS (Figure 2).

Table 1. Amino acid sequence and physicochemical properties of Hylin a1 and its analog peptides.

Name	Sequence	μH[a]	Net Charge[a]	Molecular weight (Da)		R.T (min)[b]
				Calculated	Observed	
Hylin a1	IFGAILPLALGALKNLIK-NH_2	0.473	+2	1864.4	1863.9	23.533
Hylin a1-2A	IAGAILPLALGALKNLIK-NH_2	0.393	+2	1788.3	1788.7	26.420
Hylin a1-3K	IAKAILPLALGALKNLIK-NH_2	0.420	+3	1859.4	1859.8	23.700
Hylin a1-11K	IAKAILPLALKALKNLIK-NH_2	0.471	+4	1930.5	1930.3	23.342
Hylin a1-15K	IAKAILPLALKALKKLIK-NH_2	0.482	+5	1944.4	1945.0	22.175

[a] Mean hydrophobic moments (μH) and net charge was calculated using the HeliQuest site.

[b] Retention time (min) in reversed-phase high performance liquid chromatography (RP-HPLC)

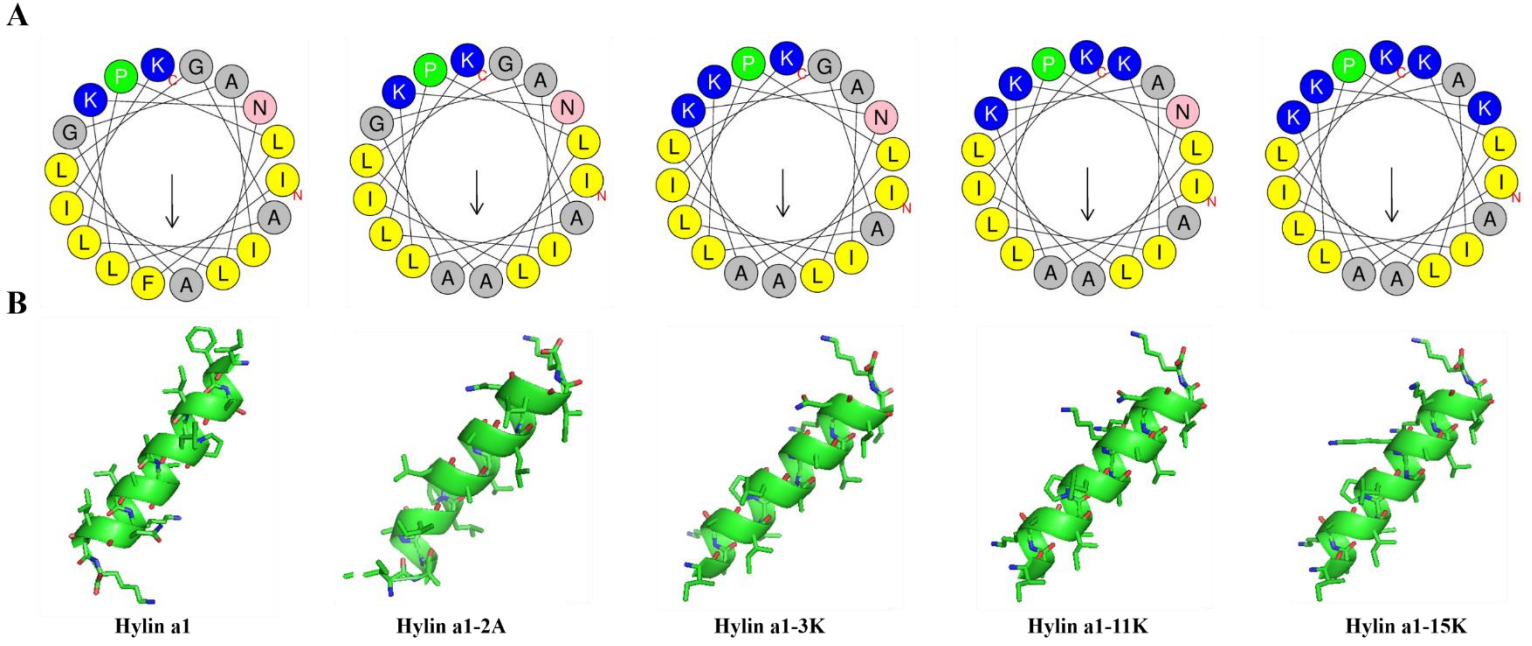

Figure 1. Structure of Hylin a1 and its analog peptides. (A) Helical wheel diagrams and (B) three-dimensional structure projections of Hylin a1, Hylin a1-2A, Hylin a1-3K, Hylin a1-11K and Hylin a1-15K were obtained from the HeliQuest site and Mobyle@RPBS portal.

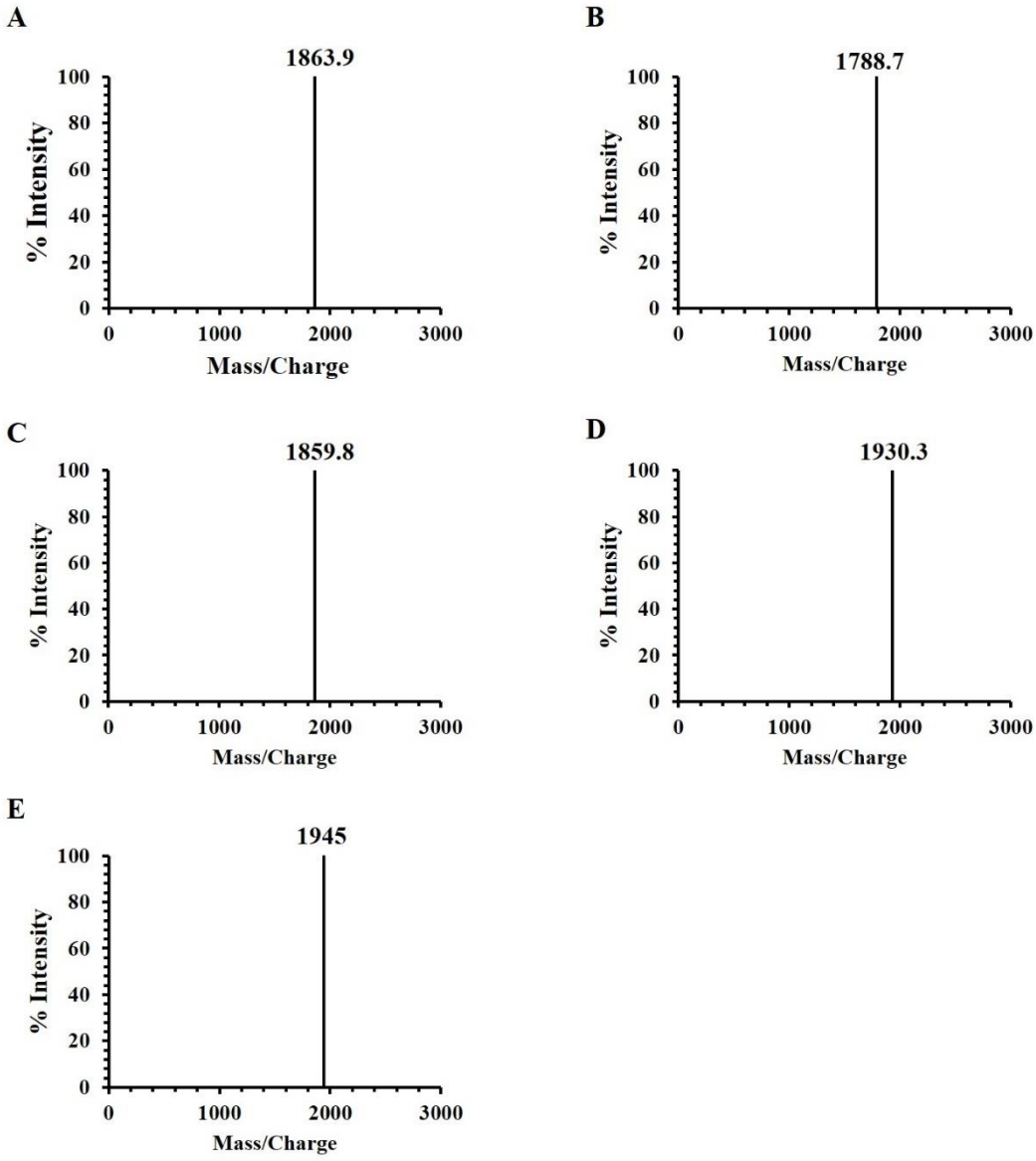

Figure 2. MALDI mass spectrometric analysis of Hylin a1 and its analog peptides. (A) Hylin a1, (B) Hylin a1-2A, (C) Hylin a1-3K, (D) Hylin a1-11K and (E) Hylin a1-15K. The mass/Charge ratio were 1863.9, 1788.7, 1859.8, 1930.3, and 1945, respectively.

2. Antimicrobial Activity of Synthetic Peptides

We confirmed the antimicrobial activity of representative Gram-negative and Gram-positive bacteria strains. In Gram-negative bacteria strains, all analog peptides were inhibited by *E. coli* and *A. baumannii*, and Hylin a1-11K and Hylin a1-15K were more effective than the parent peptides against *P. aeruginosa*. In Gram-positive bacteria strains, Hylin a1-11K and Hylin a1-15K showed antimicrobial activity against *B. cereus* and *S. typhimurium*. It also showed the most antimicrobial activity in *S. aureus* at 1-2 μM. The parent peptide and Hylin a1-2A and Hylin a1-3K showed selective activity, and Hylin a1-11K and Hylin a1-15K displayed broad-spectrum antimicrobial activity against Gram-negative and Gram-positive bacteria, as shown in Table 2.

The MICs were measured using 26 EJAB and 13 EJSA clinical isolates from the patient. The results are shown in Tables 3 and 4. The synthesized peptide showed effects on the bacteria at various concentrations, among which Hylin a1-11K and 15K demonstrated activity at a lower concentration than the parent peptide, Hylin a1.

Table 2. Antimicrobial activity of analog peptides against Gram-negative and Gram-positive bacteria strains.

Microorganisms	MIC[a] (μM)					
	Hylin a1	Hylin a1-2A	Hylin a1-3K	Hylin a1-11K	Hylin a1-15K	Melittin
Gram negative						
E coli ATCC 25922	4	16	2	2-4	1-2	1-2
P. aeruginosa ATCC 27853	>32	>32	>32	2-4	2	2
A. baumannii KCTC 2508	2	8	2-4	1-2	1-2	1-2
Gram positive						
S. aureus ATCC 25923	1	2	1	1	1	1
S. aureus ATCC 29213	2	8	4	2	1	1
B. cereus KCTC 1012	8-16	>32	4	1-2	1-2	1-2
S. typhimurium KCTC 1926	32	>32	>32	4	1-2	2-4

[a] Minimal inhibitory concentration (MIC) was determined by the growth of inhibited bacteria at the lowest peptide concentration.

Table 3. Antimicrobial activity of analog peptides against 26 EJAB strains.

Microorganisms	MIC (μM)									
	Hylin a1	Hylin a1-2A	Hylin a1-3K	Hylin a1-11K	Hylin a1-15K	Melittin	Tigecycline	Polymyxin B	Meropenem	Ceftriaxone
A. baumannii KCTC 2508	4	8	4	1-2	1-2	1	0.5	2	4	32
EJ *A. baumannii* 1	4	8	4	1-2	1-2	1-2	1	1	128	>256
EJ *A. baumannii* 2	4	8	2-4	1-2	1-2	1	2	1	256	>256
EJ *A. baumannii* 3	4	16	4	2	1-2	1-2	2	2	256	>256
EJ *A. baumannii* 4	4	8-16	2-4	1-2	1	1-2	1	1	256	>256
EJ *A. baumannii* 5	4	8	2-4	1	1	1	2	1	256	>256
EJ *A. baumannii* 6	8	16	4	1-2	1-2	1	2	0.5	128	>256
EJ *A. baumannii* 7	4	16	4	1-2	1-2	1	2	1	128	>256
EJ *A. baumannii* 8	4-8	16	4	1-2	1-2	1-2	2	1	128	>256
EJ *A. baumannii* 9	4	8	2-4	1	1-2	1	2	0.5-1	128	>256
EJ *A. baumannii* 10	4-8	16	4-8	1-2	1-2	1	2	2	128	>256
EJ *A. baumannii* 11	2-4	8	2	1-2	1-2	1	2	1	256	>256
EJ *A. baumannii* 12	4	8-16	2-4	1	1	1	4	1	64	>256
EJ *A. baumannii* 13	2-4	8	2-4	1-2	1	1	2	1	128	>256
EJ *A. baumannii* 14	4-8	16	2-4	1	1-2	1	1	1	256	>256
EJ *A. baumannii* 15	4	8	2	1-2	1	1	2	1	256	>256
EJ *A. baumannii* 16	4	8-16	2-4	1-2	1	1	2	1	128	>256
EJ *A. baumannii* 17	2-4	8	2-4	1	1	1	1	1	256	>256
EJ *A. baumannii* 18	4	8	4-2	1	1	1	2	1	128	>256
EJ *A. baumannii* 19	4-8	16	4	1-2	1	1	2	1	256	>256
EJ *A. baumannii* 20	2-4	4	2	1	1	1	2	1	256	>256
EJ *A. baumannii* 21	4	8-16	2-4	1-2	1	1	2	1	128	>256
EJ *A. baumannii* 22	4-8	8-16	2-4	1-2	1-2	1	2	1	256	>256
EJ *A. baumannii* 23	2-4	8	2-4	1	1	1	2	1	256	>256
EJ *A. baumannii* 24	4-8	16	4	1-2	1	1	2	1	128	>256
EJ *A. baumannii* 25	4	8	2	1-2	1	1	2	1	128	>256
EJ *A. baumannii* 26	4	16	4	1-2	1-2	1	2	1	256	>256

Table 4. Antimicrobial activity of analog peptides against 13 EJSA strains.

Microorganisms	MIC (μM)									
	Hylin a1	Hylin a1-2A	Hylin a1-3K	Hylin a1-11K	Hylin a1-15K	Melittin	Vancomycin	ceftriaxone	Clindamycin	Oxacillin
S. aureus ATCC 25923	1	2	1	1	1	1	0.5	4	4	4
S. aureus ATCC 29213	2	8	4	2	1	1	0.5	4	4	4
EJ *S. aureus* 1	2	4-8	8	2	1-2	1	0.5	>256	>256	>256
EJ *S. aureus* 2	2-4	8-16	8	2	1-2	1	0.5	>256	>256	>256
EJ *S. aureus* 3	2	16	8	2	1-2	1	0.5	>256	>256	>256
EJ *S. aureus* 4	2-4	32	8-16	2	1-2	1	0.5	>256	>256	>256
EJ *S. aureus* 5	2	4-8	4	2	1-2	1	0.5	>256	>256	>256
EJ *S. aureus* 6	2-4	16	8	1-2	1-2	1	0.5	>256	>256	>256
EJ *S. aureus* 7	2	8-16	4-8	2	1-2	1	0.5	>256	>256	>256
EJ *S. aureus* 8	2-4	16	8-16	2	1-2	1	0.5	>256	>256	>256
EJ *S. aureus* 9	2	8-16	8	2	1-2	1	0.5	>256	>256	>256
EJ *S. aureus* 10	2-4	16	4-8	1-2	1-2	1	0.5	>256	>256	>256
EJ *S. aureus* 11	2	8	4-8	2	1-2	1	0.5	256	>256	>256
EJ *S. aureus* 12	2-4	8-16	8	2	1-2	1	0.5	>256	>256	>256
EJ *S. aureus* 13	2	8-16	8	2	1-2	1	0.5	>256	>256	256

3. Hemolysis of Synthetic Peptides

Toxicity analysis of analog peptides was performed using sheep erythrocytes. The results of hemolysis analysis are shown in Figure 3. Melittin from bee venom, used as a positive control [18], caused approximately 100% hemolysis, and the parent peptide Hylin a1 showed 94% hemolysis at a concentration of 50 μM. The analog peptide Hylin a1-2A and Hylin a1-3K showed 3% and 15% hemolysis at 50 μM, respectively, with values of 30% and 28% for Hylin a1-11K and Hylin a1-15K, respectively. Analog peptides reduced hemolysis by 60–90% compared to parent peptides, suggesting reduced toxicity toward sRBC.

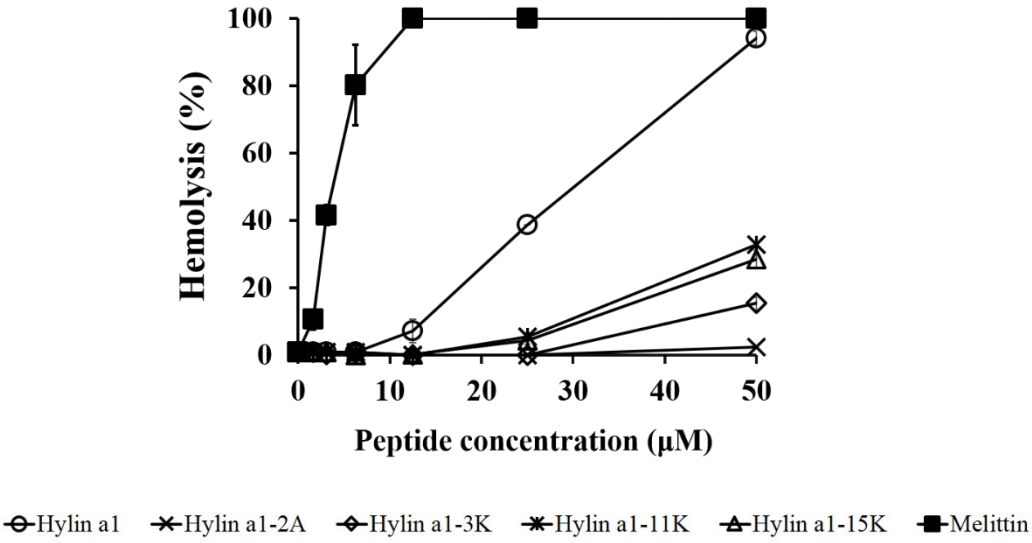

Figure 3. Hemolytic effect of analog peptides. Hemolytic rate was determined using sheep red blood cells. Various peptide concentrations (50, 25, 12.5, 6.25, 3.125, 1.56 and 0 μM) for 1h incubation. After supernatant transfer, absorbance of hemoglobin was measured at 414 nm. Melittin was used as a positive control.

4. Peptide Structure in Various Solution Environments

We performed CD spectroscopy to determine the structures of the analog peptides in various solutions. The α-helix structure was evaluated based on Figure 2, with 10 mM sodium phosphate buffer (to simulate the aqueous environment), 30 mM SDS (to simulate the cationic environment of the bacterial membrane), and 50% TFE (to simulate the hydrophobic environment of the microbial membrane) used to dissolve each 40 μM of parent peptide and analog peptides. The result is shown in Figure 4. Parent peptides and analog peptides exhibited random coil structures (very low ellipticity above 210 nm and negative bands near 195 nm) in 10 mM sodium phosphate buffer. However, α-helix structures (negative bands at 222 and 208 nm and positive bands at 193 nm) appeared in the biomimetic solution, 30 mM SDS, and 50% TFE. In a previous study, Hylin a1 showed consistent results with the α-helix structure at 60% TFE. The Hylin a1 and analog peptides showed alpha-helix structures in the biomimetics, as expected.

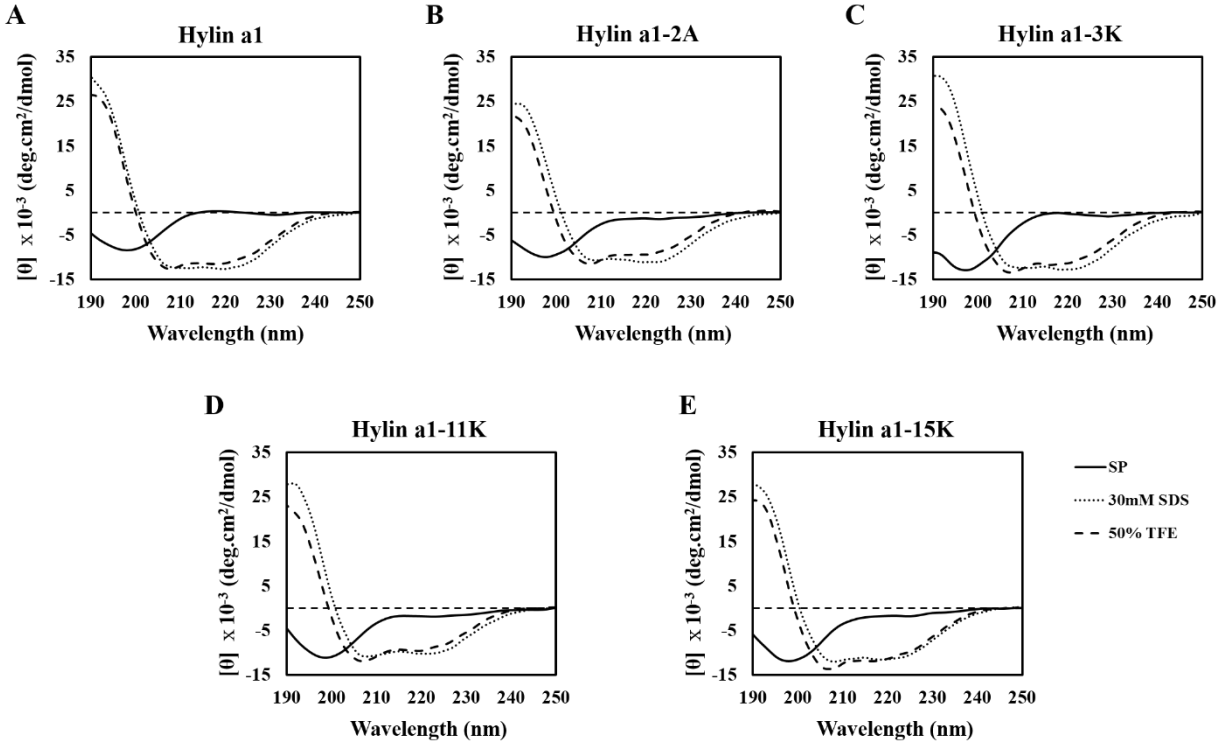

Figure 4. Circular dichroism (CD) spectroscopy measurements of (A) Hylin a1, (B) Hylin a1-2A, (C) Hylin a1-3K, (D) Hylin a1-11K, and (E) Hylin a1-15K. The peptides were dissolved in 10 mM sodium phosphate buffer (to simulate the aqueous environment), 30 mM SDS (to simulate the cationic environment of the bacterial membrane), or 50% 2,2,2-trifluoroethanol (TFE) (to simulate the hydrophobic environment of the microbial membrane). The peptides concentration was fixed to 40 μM.

5. Biological Activity of Analog Peptides

To evaluate whether the biofilm was inhibited, a crystal violet assay was performed [19]. Biofilms were formed from *A. baumannii* strains to evaluate EJAB 10 and EJAB 24 (Figure 5A). In case of the *A. baumannii* KCTC 2508, the biofilm formation rate of Hylin a1, Hylin a1-2A, Hylin a1-3K, Hylin a1-11K, and Hylin a1-15K were 85%, 78%, 54%, 9%, and 15% at 4 μM, respectively (Figure 5B). The resistant strains EJAB 10 and EJAB 24 showed 14% and 6% biofilm formation of Hylin a1-11K and Hylin a1-15K, respectively, at 4 μM (Figure 5C and D). Analog peptides showed higher he biofilm inhibition activity than the parent peptides.

Figure 6 shows the biofilm formation of *S. aureus* strains and peptide of biofilm inhibition activity against the bacteria. The resistant strains EJSA 5 and EJSA 11 showed the highest biofilm formation (Figure 6A). In the case of *S. aureus* ATCC 25923, the parent peptide and analog peptide showed biofilm removal activity at 2–4 μM (Figure 6B). In the resistant strains EJSA 5 and EJSA 11, Hylin a1, Hylin a1-11K, and Hylin a1-15K showed approximately 5% biofilm formation at 8 μM.

We formed bacteria for 24 h to confirm the biofilm reduction susceptibility of the peptide, and then treated the peptide to confirm the biofilm reduction activity. The parent peptide and analog peptide were treated from 0 to 128 μM, and after 24 h, crystal violet staining analysis was performed. The results are shown in Figure 7. The biofilm reduction activity of the analog peptides were evaluated for *A. baumannii* KCTC 2508, EJAB 10, and EJAB 24 and *S. aureus* ATCC 25923, EJSA 5, and EJSA 11.

The maximum percentage of biofilm reduction by Hylin a1 and its analog peptides (Hylin a1-11K and Hylin a1-15K) for *A. baumannii strains* were 47%, 49%, and 66% against *A. baumannii* KCTC 2508, 40%, 50%, and 65% against EJAB 10, and 11%, 32%, and 23% against EJAB 24) at all peptide concentrations (32 μM), respectively (Figure 7A–C). Additionally, *S. aureus* ATCC

25923 showed biofilm reductions of 71%, 72%, and 65%, EJSA 5 showed reductions of 12%, 47%, and 61%, and EJSA 11 showed reductions of 53%, 62%, and 69% (Figure 7D–F).

The biofilm reduction effect of the parent peptide and analog peptides was quantified as the maximum percentage. Biofilms were visualized by fluorescence using SYTO 9 (green dye) to detect live cells [20]. SYTO 9 dye distinguishes live and dead cells and stains Gram-negative bacteria and Gram-positive bacteria in bacterial assays. Standard and MDR strains were cleaved by analog peptides. Particularly, the fluorescence was effectively lowered at 32 and 64 μM by Hylin a1-11K and Hylin a1-15K, respectively. The results are shown in Figure 8.

These results demonstrate that analog peptides effectively removed biofilms against standard strains (*A. baumannii* KCTC 2508 and *S. aureus* ATCC 25923) and MDR strains (EJAB 10, EJAB 24, EJSA 5, and EJSA 11).

To determine the killing rate of Hylin a1 and analog peptides against *A. baumannii* and *S. aureus*, the peptides and bacteria were treated simultaneously and then evaluated at different times (5, 10, 15, 30, 45, 60, 90, and 120 min). As shown in Figure 9, the parent peptide, Hylin a1, did not completely kill the bacteria at 1x MIC against *A. baumannii* and *S. aureus*, but rather showed an increasing pattern. In contrast, Hylin a1-11K and Hylin a1-15K killed the bacteria within 5 min at all concentrations. These peptides also acted very rapidly on all bacteria at the inhibitory concentrations.

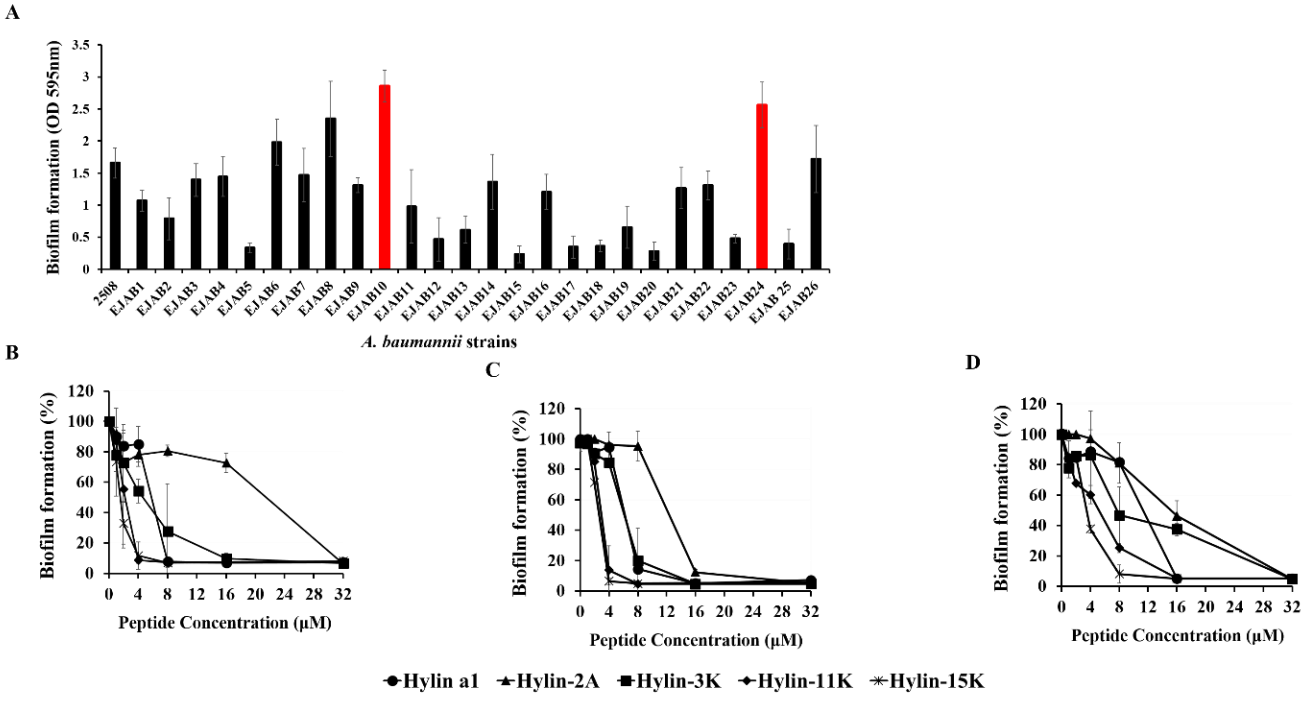

Figure 5. Biofilm formation and inhibition assay. (A) Formation and quantification of biofilms by clinical isolates of *A. baumannii* (26 strains). (B) Standard strain *A. baumannii* KCTC 2508, (C) EJ *A. baumannii* 10, and (D) EJ *A. baumannii* 24. Inhibition of biofilm formation by Hylin a1, Hylin a1-2A, Hylin a1-3K, Hylin a1-11K, and Hylin a1-15K against the microorganisms. Each well contained 50 μL of 5×10^5 CFU/mL suspension of bacteria. The biofilms were then stained with crystal violet and absorbance was measured at 595 nm.

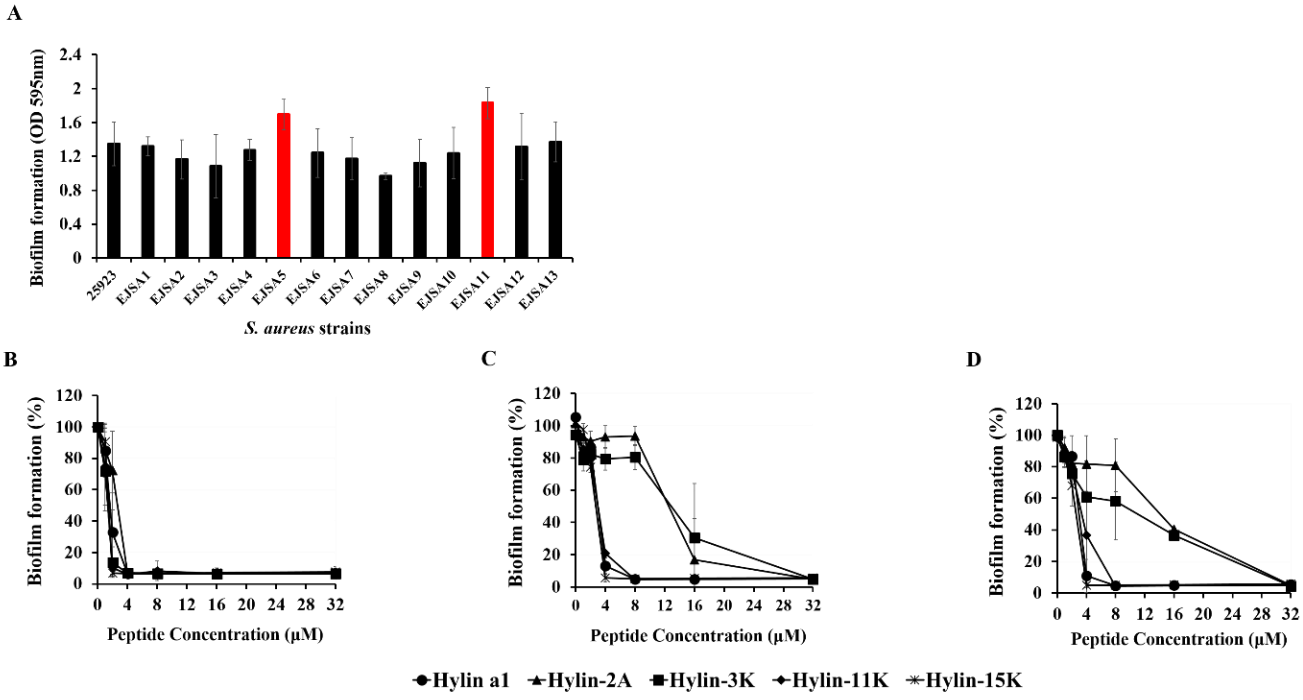

Figure 6. Biofilm formation and inhibition assay. (A) Formation and quantification of biofilms by clinical isolates of *S. aureus* (13 strains). (B) Standard strain *S. aureus* ATCC 25923, (C) EJ *S. aureus* 5, and (D) EJ *S. aureus* 11. Inhibition of biofilm formation by Hylin a1, Hylin a1-2A, Hylin a1-3K, Hylin a1-11K, and Hylin a1-15K against the microorganisms. Each well contained 50 μL of 5×10^5 CFU/mL suspension of bacteria. The biofilms were then stained with crystal violet and absorbance was measured at 595 nm.

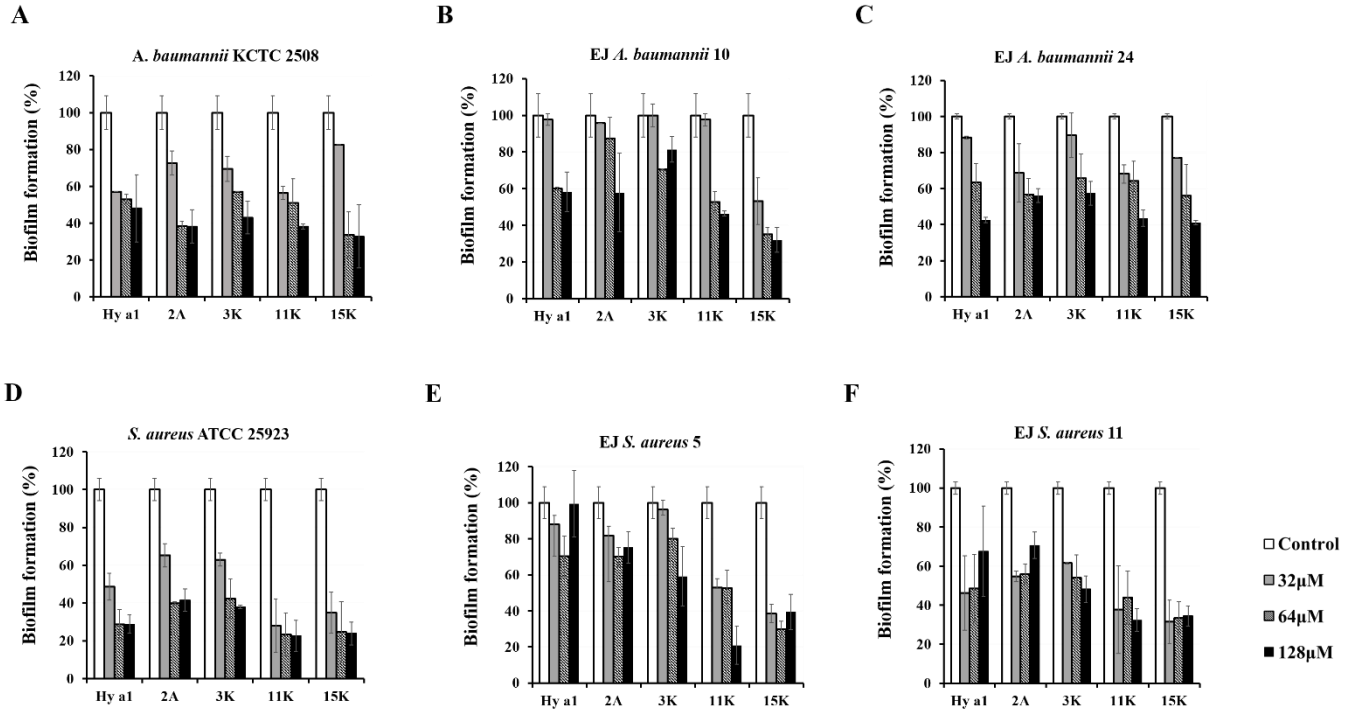

Figure 7. Biofilm reduction assay. Bacteria were cultured for 24 h at 37°C. Next, the peptides were treated at concentrations of 32–128 μM, and the biofilm was stained with crystal violet and quantified at 595 nm. (A) *Acinetobacter baumannii* KCTC 2508, (B) EJAB 10, (C) EJAB 24, (D) *S. aureus* ATCC 25923, (E) EJSA 5, and (F) EJSA 11.

A

A. baumannii **KCTC 2508**

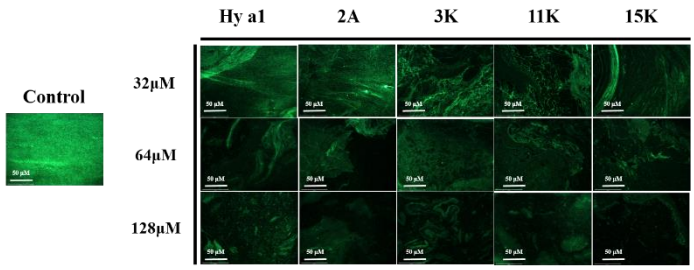

B

EJ ***A. baumannii 10***

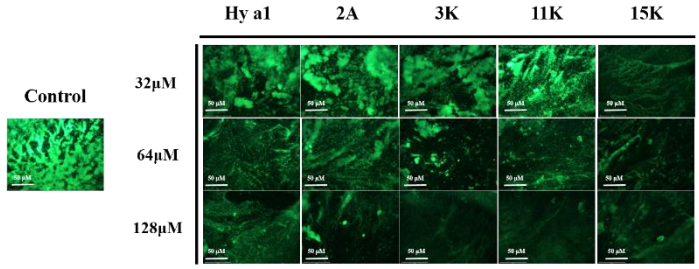

C

EJ ***A. baumannii*** **24**

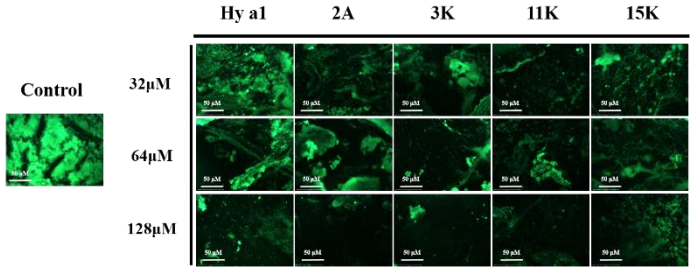

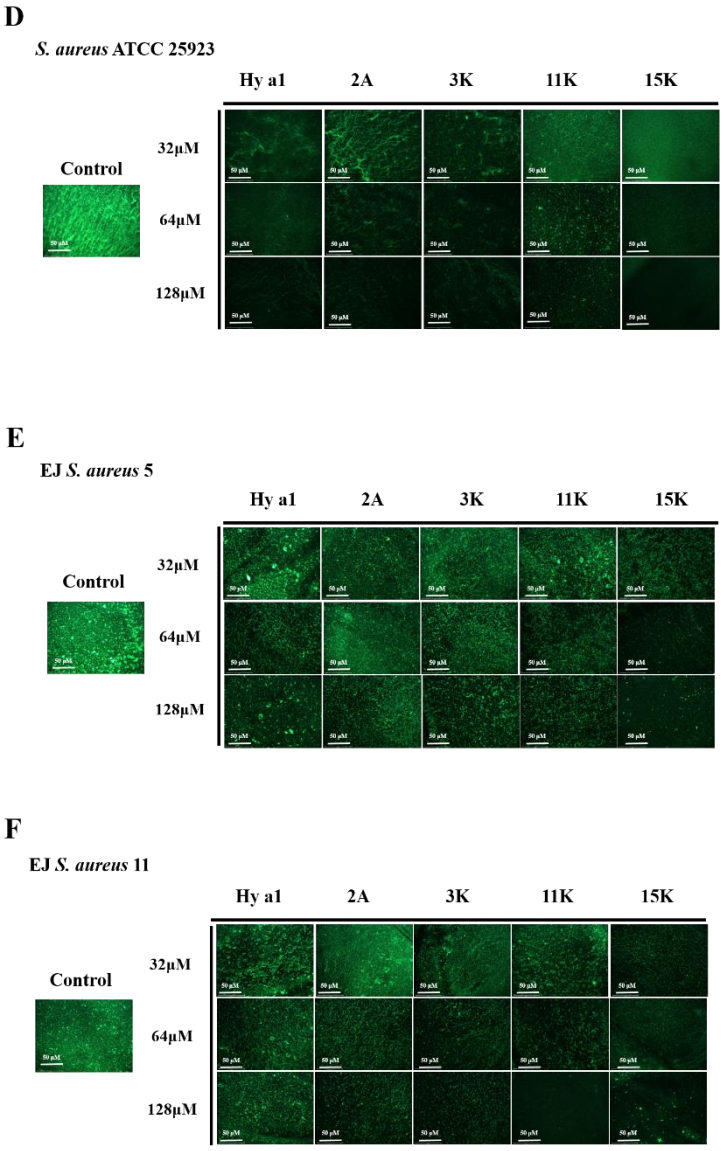

Figure 8. Biofilm reduction visualization analysis. After biofilm formation by microorganisms for 24 h at 37°C, peptides were used to treat the cells at concentrations of 32, 64, and 128 μM. Controls contained only bacteria. Live cells were evaluated using EVOS by staining with SYTO 9 (green dye). (A) *A. baumannii* KCTC 2508, (B) EJAB 10, (C) EJB 24, (D) *S. aureus* ATCC 25923, (E) EJSA 5, and (F) EJSA 11. Scale bar = 50 μM.

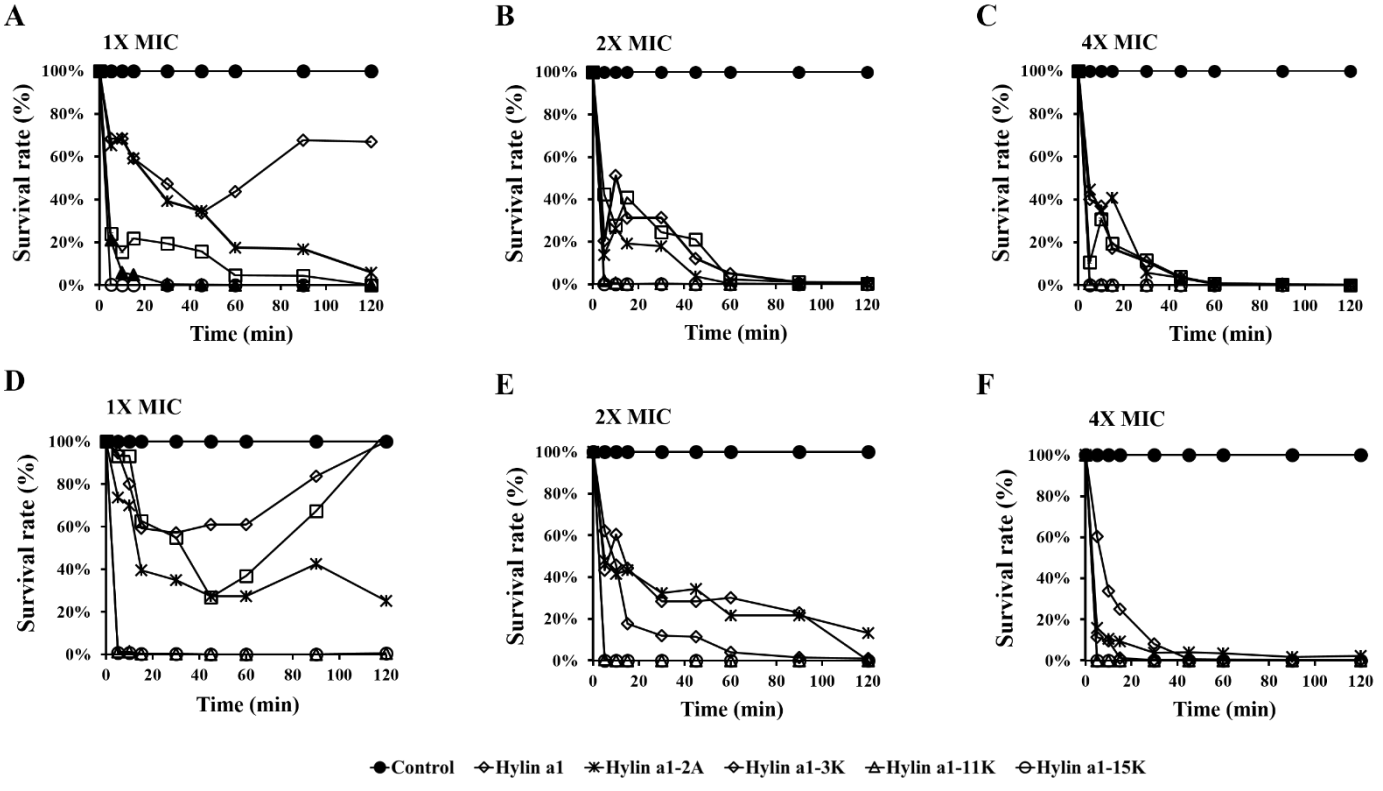

Figure 9. Time kinetics assay. (A–C) *A. baumannii* KCTC 2508 and (D–F) *S. aureus* ATCC 25923. Bactericidal kinetics of Hylin a1 and its analog peptides were examined at different peptide concentrations (1x, 2x, and 4x MIC). Bacteria (2×10^5 CFU/mL) and peptides were treated together and then evaluated at different times (min).

6. Stability Activity of Peptides

The antimicrobial activity of the peptides at physiological cation concentrations was confirmed by the MIC method. The effects of the peptides on *A. baumannii* KCTC 2508 and *S. aureus* ATCC 25923 were confirmed by addition of monovalent ions (NaCl), divalent ions ($MgCl_2$), and trivalent ions ($FeCl_3$). The effect of peptides on *A. baumannii* KCTC 2508 was 2–16-fold lower than the original MIC values of the parent peptide and Hylin a1-2A and Hylin a1-3k of monovalent (NaCl) and trivalent ions ($FeCl_3$), and Hylin a1-11k and Hylin a1 -15k was maintained or reduced by 2-fold. Higher concentrations of divalent ions ($MgCl_2$) led to lower activities of the parent peptide, Hylin a1-2A, and Hylin a1-3k, even at concentrations above 32 μM. At 0.5, 1, and 2 mM divalent ions ($MgCl_2$), the antimicrobial activities of 4, 4, and 8 μM Hylin a1-11K and 8, 16, and 32 μM Hylin a1-15K were evaluated. In the case of *S. aureus* ATCC 25923, the antimicrobial activities of the peptides at all concentrations of cations were decreased or maintained at 2-fold of the MIC value (Table 5).

To determine peptide stability in human serum, the antimicrobial activity of the peptides in human serum was measured. Because peptide-based drugs are sensitive to proteases, the antimicrobial effects in human serum were analyzed. Peptide effects on standard strains (*A. baumannii* KCTC 2508 and *S. aureus* ATCC 25923) and MDR strains (EJAB 10, EJSA 11) were measured after 18 h of treatment in 5% and 10% human serum. The antimicrobial effect of the peptides on *A. baumannii* KCTC 2508 and EJAB 10 were higher for Hylin a1-11K and Hylin a1-15K than the parent peptides in 5% and 10% human serum. Additionally, strong antimicrobial effects against *S. aureus* ATCC 25923 and EJSA 10 were observed. The analog peptides were not affected by human serum and demonstrated antimicrobial effects (Table 6).

Table 5. MIC value of Hylin a1 and its analog peptides on bacteria strains at various cation concentrations.

Salt	Concentration	*A. baumannii* KCTC 2508					*S. aureus* ATCC 25923				
		Hylin a1	Hylin a1-2A	Hylin a1-3K	Hylin a1-11K	Hylin a1-15K	Hylin a1	Hylin a1-2A	Hylin a1-3K	Hylin a1-11K	Hylin a1-15K
NaCl	**50mM**	8	32	8	2	4	2	4	2	2	2
	100mM	8	32	16	4	2	2	4	4	2	2
	150mM	8	>32	32	4	2	2	4	4	2	2
$MgCl_2$	**0.5 mM**	16	>32	>32	8	4	2	4	2	2	2
	1 mM	32	>32	>32	16	4	2	4	4	2	2
	2 mM	>32	>32	>32	32	8	4	8	4	2	2
$FeCl_3$	**2 μM**	4	16	8	4	4	2	2	4	2	2
	4 μM	4	8	4	4	2	2	2	2	2	2
	8 μM	4	8	4	4	4	2	4	4	2	2

Table 6. MIC values of Hylin a1 and its analog peptides against bacteria in 5% and 10% human serum

Microorganisms	5% Serum					10% Serum				
	Hylin a1	Hylin a1-2A	Hylin a1-3K	Hylin a1-11K	Hylin a1-15K	Hylin a1	Hylin a1-2A	Hylin a1-3K	Hylin a1-11K	Hylin a1-15K
***A. baumannii* KCTC 2508**	8	32	32	2	4	64	32-64	64	4-8	8
***S. aureus* ATCC 25923**	8	16	16	1	1	4-16	16-32	64	2	1
EJAB 10	16	64	64	4	16	32-64	64	64	8	32
EJSA 11	4	16	64	8	4	8	16-32	64	8	4

7. Liposome Calcein Leakage Activity

To assess the membrane permeability of the peptide, large unilamellar vesicles (LUVs) containing calcein were used for leakage analysis. Encapsulation of calcein in liposomes does not measure fluorescence, but calcein release of liposomes due to peptide induction shows strong fluorescence. Based on this, each vesicle was treated with a peptide to confirm the permeability of the membrane. Liposomes mimic PC: CH to mimic erythrocyte membranes, and PE: PG mimic bacterial membranes. Liposomes were prepared, and the parent peptide and analog peptides were treated according to various peptide/liposome ratios (0.2, 0.1, and 0.05). The results are shown in Figure 9.

The effect of peptides on PC: CH vesicles was measured to measure calcein release activity (Figure 9A). Melittin was used as a positive control and Buforin-2 was used as a negative control. The parent peptide showed a calcein release of 150% at P/L 0.2, similarly to the positive control melittin. For Hylin a1-2A, Hylin a1-3K, Hylin a1-11K, and Hylin a1-15K, the release rates were 7%, 7%, 57%, and 69%, respectively (Figure 9A). These results showed that similar peptides did not affect the mammalian membranes more than the parent peptides. Gram-negative bacteria membrane PE: PG vesicles, parent peptide, and Hylin a1-11K and Hylin a1-15K showed calcein release rates of 49%, 59%, and 117%, respectively (Figure 9B). The effects of the peptides on PE: PG vesicles confirmed the potent effects on the bacterial membranes.

Calcein leakage was observed using a FOBI. Hylin a1 showed calcein leakage activity like the positive control Melittin in PC:CH liposomes. The intensity of the analog peptide was lower than that of the parent peptide (Figure 10A). PE: PG showed stronger release of calcein induced by peptides in Hylin a1-11K and Hylin a1-15K than Hylin a1. These results suggest that the analog peptides had lower effects on PC: CH, but they did not strongly affect PE: PG.

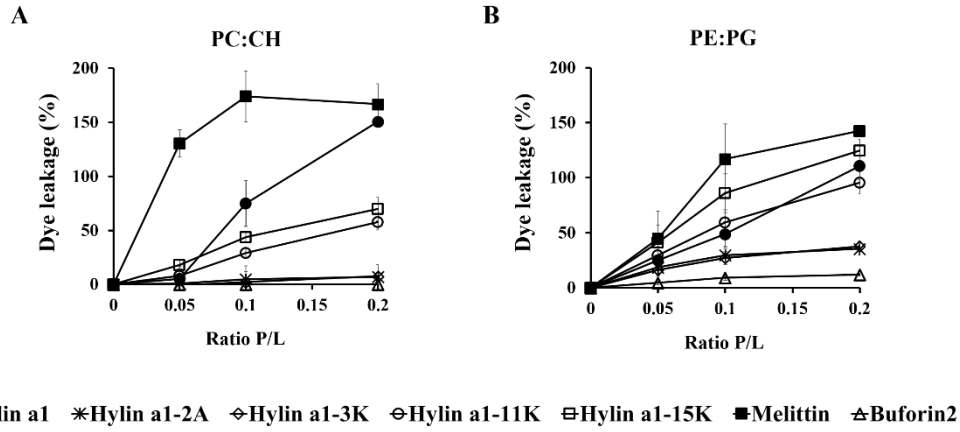

Figure 10. Calcein leakage assay. Calcein measurements were performed with various peptide/liposome ratios (0.2, 0.1, and 0.05). Increased calcein leakage was detected in 10 μM of (A) PC:CH (2:1, w/w), (B) PE:PG (7:3, w/w) LUVs.

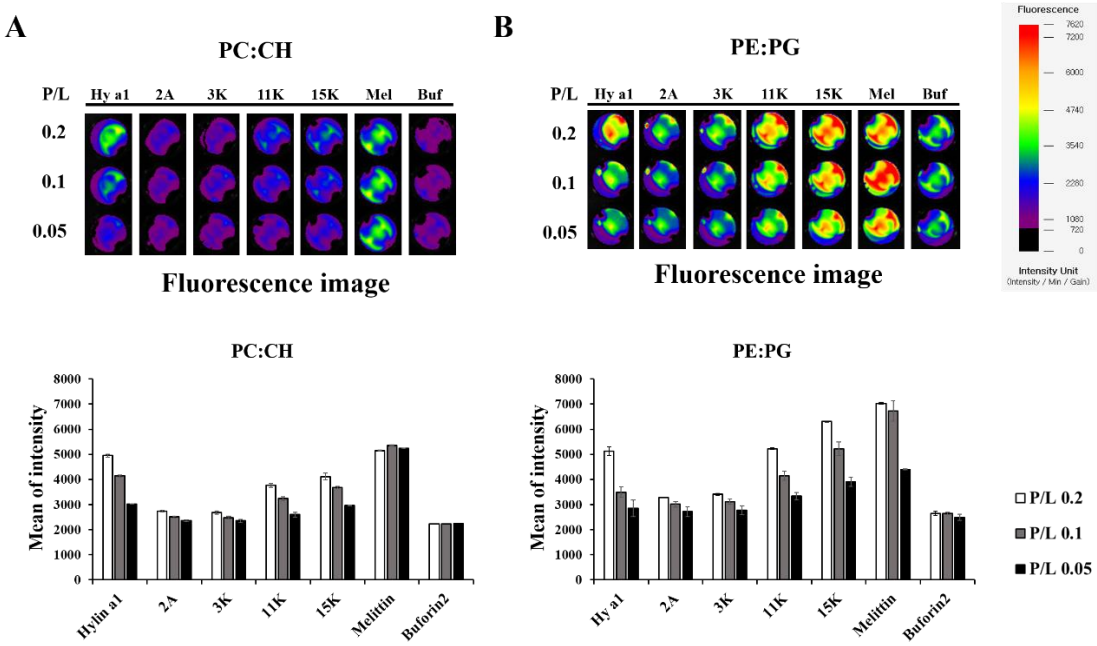

Figure 11. Visualization of liposome calcein leakage, (A and B) images indicate fluorescence of calcein leakage in liposomes using fluorescence-labeled organism bioimaging instrument. PC:CH (2:1, w/w) and PE:PG (7:3, w/w) LUVs were treated at various concentrations (P/L 0.2, 0.1, and 0.05). Quantification was performed by measuring calcein leakage strength.

8. Action of Mechanism of Analog Peptides

We used NPN, ONPG, diSC$_3$-5, SYTOX green, and PI to determine the mechanism by which peptides target bacterial membranes. In this study, bacterial membranes were targeted and detected as the release of fluorescence inside the outer and inner membranes or inside the cells. The hydrophobic fluorescent dye NPN recognizes and reverses external and internal charges in bacteria. As shown in Figure 11, the peptides were treated with *A. baumannii* KCTC 2508 and *S. aureus* ATCC 25923 at 4x, 2x, and 1x MIC to confirm the increased fluorescence levels. Hylin a1 and its analog peptides affected the bacterial outer membrane and induced the fluorescence of NPN.

ONPG confirmed the effect of peptides on the production of beta-galactosidase from *E. coli*. ONPG is expressed in the cytoplasmic space between the bacterial outer membrane and the inner membrane and can be classified into two residues when the peptide was added to confirm the permeability of the inner membrane. As shown in Figure 12, the peptides penetrated the inner membrane in a concentration-dependent manner against *E. coli* expressing ONPG. All peptides showed strong effects from 10 to 20 min.

Membrane depolarization analysis was performed using diSC$_3$-5. The bacterial cytoplasmic membrane diSC$_3$-5 is a voltage-sensitive dye, acting as a potentiometric probe. The dye accumulates in the membrane and displaces into the lipid bilayer. As shown in Figure 13. *A. baumannii* KCTC 2508 and *S. aureus* ATCC 25923 were treated at 4x, 2x, and 1x MIC peptide concentrations for 60 min. All peptides induced depolarization of the membrane. Additionally, the effects of Hylin a1-11K and Hylin a1-15K on *S. aureus* ATCC 25923 were higher than those of other analog peptides.

We also evaluated the complete permeation of the cell membrane using SYTOX green [21]. SYTOX green is an inherently non-fluorescent cell impermeable dye that, when the cells are damaged and divides, binds to the base of the nucleic acid in the cell and fluoresces. As shown in Figure 14, the fluorescence of SYTOX green induced by Hylin a1, Hylin a1-2A Hylin a1-3K, Hylin

a1-11K, and Hylin a1-15K was measured for 1 h. The results showed that all peptides had similar relative luminescence values of SYTOX green at 4x, 2x and 1x MIC peptides, and were induced quickly and strongly. This confirmed that all peptides completely cleaved the membrane.

We also confirmed the uptake of PI by flow cytometry. PI is a cell impermeable dye, similar to SYTOX green, and can label damaged cells. As shown in Figure 15, Hylin a1, Hylin a1-2A, Hylin a1-3K, Hylin a11K, and Hylin a1-15K were treated with PI and bacteria for 10 min, and flow cytometry was performed to detect PI. All peptides were treated at 1x MIC peptide. Bacteria containing only PI were used as a control, and the survival rate was 95.65% for *A. baumannii* KCTC 2508. Hylin a1, Hylin a1-2A, Hylin a1-3K, Hylin a1-11K, and Hylin a1-15K showed cell damage rates of 81.01%, 90.71%, 27.20%, 88.24%, and 98.01%, respectively. Additionally, *S. aureus* ATCC 25923 showed 97.71% survival, whereas Hylin a1, Hylin a1-2A, Hylin a1-3K, Hylin a1-11K, and Hylin a1-15K showed cell damage rates of 98.24%, 72.93%, 97.75%, and 98.12%, respectively. The mechanism was similar to that of the membrane target peptide control melittin [22], demonstrating that the peptide targets the membrane and strongly induces cell damage and death.

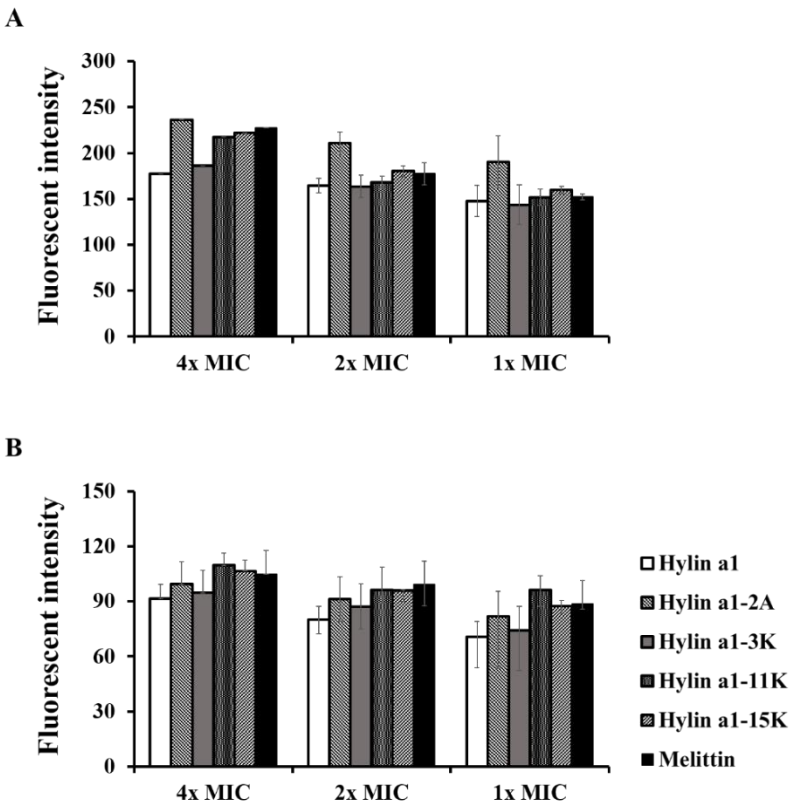

Figure 12. Outer membrane permeability assay. Permeability of outer membrane analog peptides against *A. baumannii* KCTC 2508 and *S. aureus* ATCC 25923 at 4x, 2x, and 1x MIC. Uptake of NPN fluorescence was measured at an excitation of 350 nm and emission of 420 nm. (A) *A. baumannii* KCTC 2508 and (B) *S. aureus* ATCC 25923.

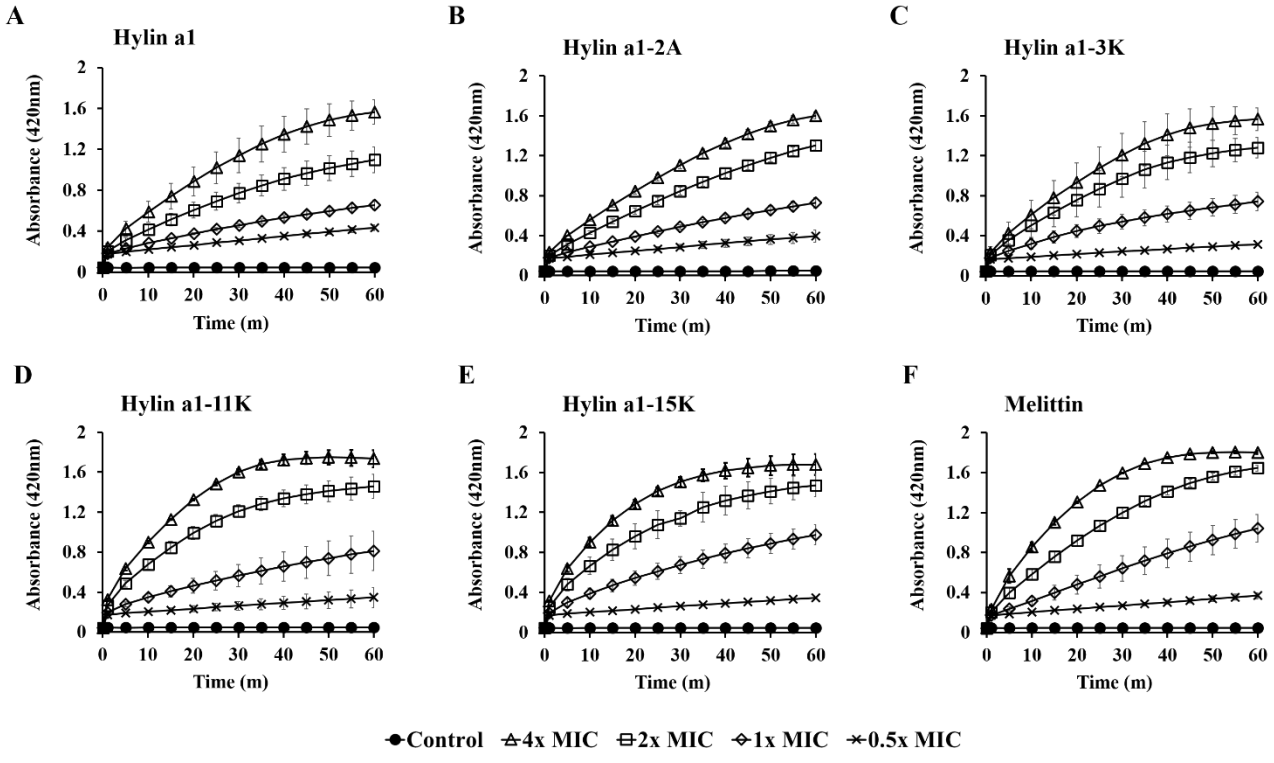

Figure 13. Inner membrane permeability assay. β-Galactosidase induction of inner membrane of *E. coli* by analog peptides. Measurement of ONPG hydrolysis rate for 60 min at 4x, 2x, and 1x MIC. (A) Hylin a1, (B) Hylin a1-2A, (C) Hylin a1-3K, (D) Hylin a1-11K, (E) Hylin a1-15K, and positive control (F) Melittin.

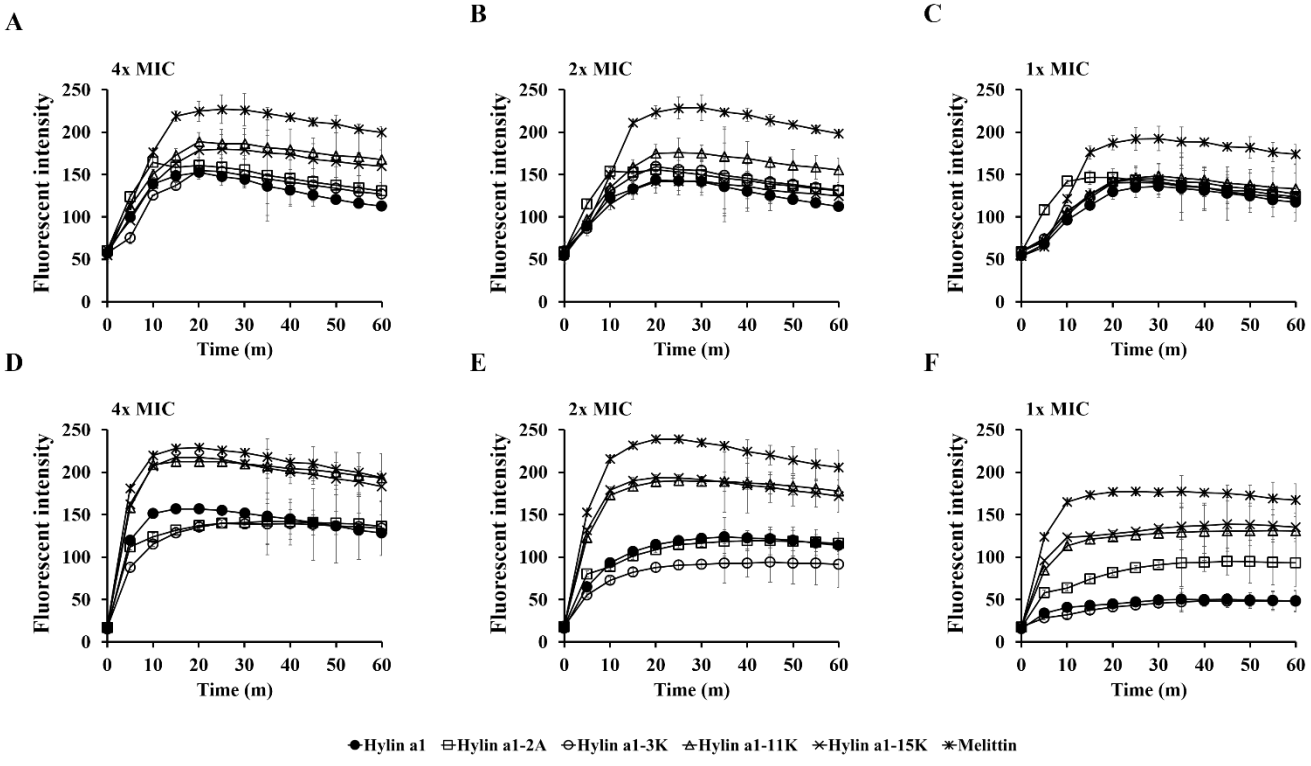

Figure 14. Cytoplasmic depolarization assay. Measurement of uptake of voltage sensitive dye $diSC_3$-5 of cytoplasmic depolarization of *A. baumannii* KCTC 2508 and *S. aureus* ATCC 25923 by analog peptides for 60 min. (A–C) Peptide concentrations at 4x, 2x, and 1x MIC on *A. baumannii*; (D–F) peptide concentration 4x, 2x, and 1x MIC on *S. aureus.*

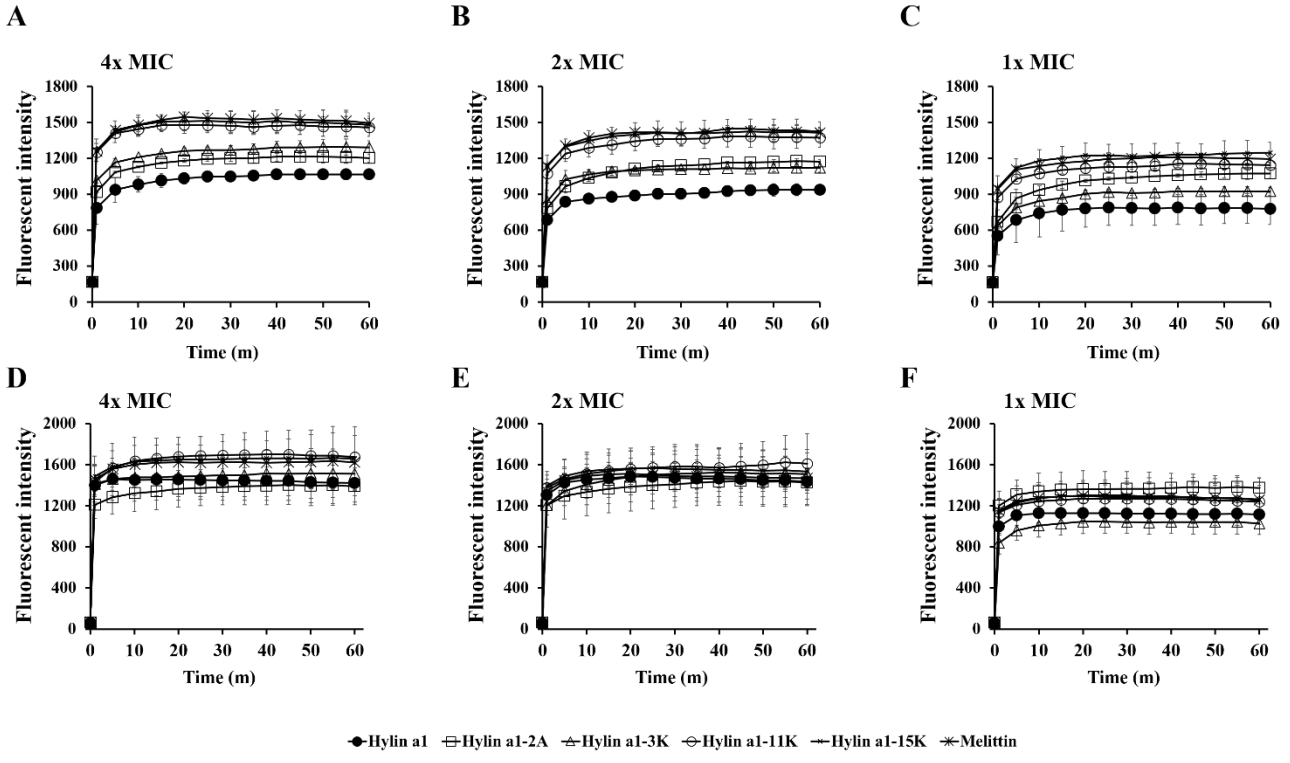

Figure 15. SYTOX green uptake assay. Measurement of fluorescence absorption uptake from (A–C) *A. baumannii* KCTC 2508 and (D–F) *S. aureus* ATCC 25923 dead cells of SYTOX green dye. Hylin a1 and analog peptides were treated at 4x, 2x, and 1x MIC peptides.

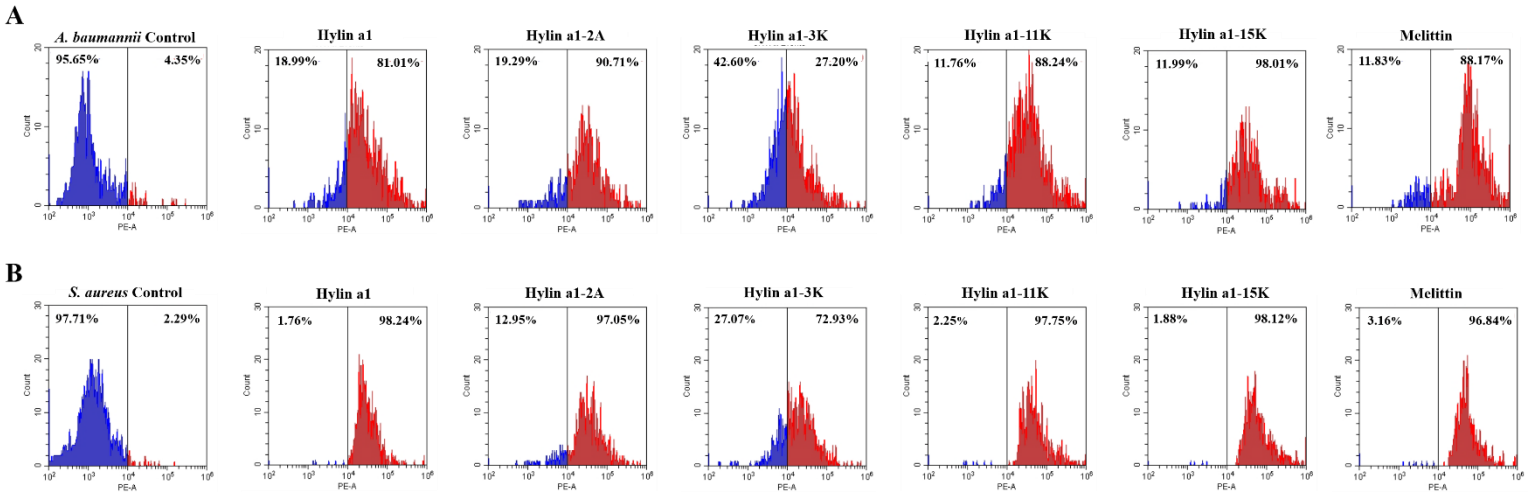

Figure 16. Flow cytometry assay. Membrane permeability was detected by evaluating (A) *A. baumannii* KCTC 2508 and (B) *S. aureus* ATCC 25923 with increased PI fluorescence by analog peptides. Controls treated with only bacteria and PI.

9. CD Spectra Analysis of LPS, LTA

We determined the CD spectrum using components of the outer membrane to ensure that the peptides were fully interact in the bacterial membrane and interfered with its integrity. LPS on the outer membrane of Gram-negative bacteria and LTA on the cell walls of Gram-positive bacteria are the major membrane components. LPS and LTA are virulence factors that protect bacteria, infect mammalian cells, and induce immune responses [20, 21].

Therefore, the ability of analog peptides to bind LPS and LTA was analyzed by structural analysis. As shown in Figure 16A, the binding structure of the peptides to LPS of *E. coli* showed a random coil structure (very low ellipticity above 210 nm and negative bands near 195 nm) for LPS for Hylin a1-2A and Hylin a1-3K. Hylin a1 11K and Hylin a1-15K showed the same α-helix structure (negative bands at 222 and 208 nm and positive bands at 193 nm). In the LTA of *S. aureus*, all analog peptides showed an α-helix structure (Table 16B). Based on these results, Hylin a1-2A and Hylin a1-3K selectively bound to LTA and did not interact with LPS. However, Hylin a1-11K and Hylin a1-15K bound to both LPS and LTA and showed an alpha helix structure.

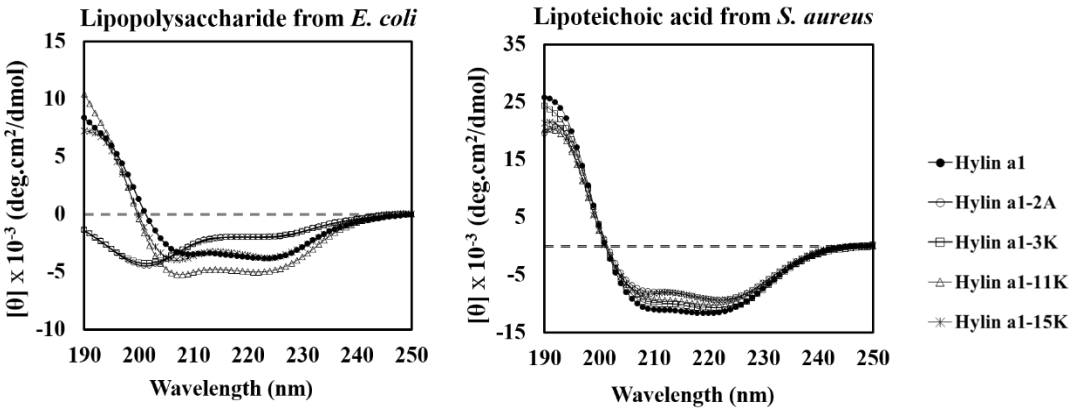

Figure 17. CD spectrum measurement of LPS and LTA. Binding affinity of the peptide for LPS of *E. coli* and LTA of *S. aureus* as measured by CD spectroscopy. The peptides (40 μM) were measured in the presence of 200 μg/mL of LPS and 500 μg/mL LTA.

10. Anti-Inflammation Effect of Analog Peptide

We determined whether peptides could inhibit the expression of pro-inflammatory cytokines when macrophages in mice were infected with bacteria. After infection with EJAB 10 in Raw264.7 cells, Hylin a1-11K and Hylin a1-15K were treated at concentrations of 0.5x MIC and 0.1x MIC after 1 h. After 10 hours, the cells were harvested, RNA was isolated and synthesized with cDNA, and then the relative expression level of mRNA was confirmed by RT-qPCR. As a result, the expression of inflammatory factors (TNF-α, IL-6 and IL-1β) was high in the infected cell population. In contrast, in the groups treated with Hylin a1-11K and Hylin a1-15K, the expression of pro-inflammatory cytokine was significantly lower. The increase in pro-inflammatory cytokine expression in Raw264.7 cells infected with EJAB 10 could modulate the mediators of inflammatory responses by treating analog peptides.

Table 7. qPCR Primers used in this study.

Gene	Primer	Sequence (5'→3')
β-actin	β-actin-F	TGGAATCCTGTGGCATCCATGAAAC
	β-actin-R	TAAAACGCAGCTCAGTAACAGTCCG
TNF-α	TNF-α-F	GGCAGGTCTACTTTGGAGTCATTGC
	TNF-α-R	ACATTCGAGGCTCCAGTGAATTCGG
IL-6	IL-6-F	CTGGTGACAACCACGGCCTTCCCTA
	IL-6-R	ATGCTTAGGCATAACGCACTAGGTT
IL-1β	IL-1β-F	TCATGGGATGATGATGATAACCTGCT
	IL-1β-R	CCCATACTTTAGGAAGACACGGATT

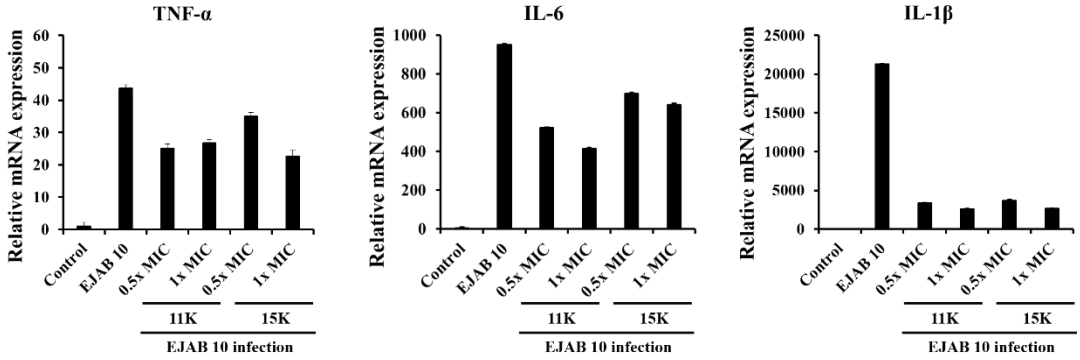

Figure 18. Effect of Hylin a1-11K and Hylin a1-15K on inflammation of EJAB 10-infected RAW264.7 cells. After 1 h, Hylin a1-11K and Hylin a1-15K were used to treat the infected cells at 0.5x and 1x MIC. Relative expression levels of the indicated inflammation-related genes in EJAB 10-infected Raw264.7 (A) TNF-α, (B) IL-6, and (C) IL-1β.

IV. Discussion

The MDR strains of *A. baumannii* [22] and *S. aureus* [23] are opportunistic pathogens that can cause serious hospital-associated infections. In the clinic, MDR bacterial infections can lead to pneumonia, septic shock, sepsis and death [24]. The potential for MDR organisms to attach to surfaces, form biofilms, and increase the ability to acquire genetic substance various resistance mechanisms and bacterial interactions is rising [25]. To overcome these factors, new non-antibiotic treatments are urgently needed [26]. AMPs are currently good candidates for treating antibiotic-resistant bacteria. AMPs have been reported as essential for innate immune elements and are active against microorganisms such as bacteria and fungi. We designed four analog peptides (Hylin a1-2A, Hylin 1-3K, Hylin a1-11K and Hylin a1-15K) based on the residues of the novel peptide Hylin a1, derived from an arboreal South American frog. This peptide is 18 amino acids and alanine (A) and lysine (K) were inserted to replace phenylalanine (F) and glycine (G) (Table 1). Ala is a hydrophobic side chain and Lys acts as an electrically charged side chain. This induces net charges from +2 to +5 and increases net charge interactions with hydrophobic bacterial membranes, reducing antimicrobial activity and toxicity in host cells [27]. We confirmed that the parent peptides and analog peptides had antimicrobial activity against Gram-negative and Gram-positive bacteria, as well as MDR strains. *A. baumannii* was designated as a representative strain in Gram-negative bacteria, and *S. aureus* was selected for Gram-positive bacteria. Antimicrobial activity was confirmed against clinical isolates *A. baumannii* (EJAB 1–26) and S. aureus (EJSA 1–13) isolated from patients at EULJI Hospital (Table 3 and 4). In a previous study, the parent peptide Hylin a1 showed broad spectrum activity in all strains, and the analog peptides Hylin a1-11K and Hylin a1-15K showed equal or better effects than the parent peptides. However, the hemolytic activity of Hylin a1 on erythrocytes was higher than that of other analog peptides (Figure 3). Our results suggest that analog peptides have antimicrobial activity and no hemolytic activity, which can be used as a safer treatment than parent peptide. Our study analyzed the secondary structure of analog peptides in solutions of SP buffer (to simulate the aqueous

environment), SDS (to simulate the cationic environment of the bacterial membrane) and TFE (to simulate the hydrophobic environment of the microbial membrane). In a previous study, Hylin a1, showed a full alpha helix structure at 60% TFE, The analog peptide showed a random coil structure in an aqueous environment as shown by the increase in the net charge, confirming that the analog peptide was folded into an alpha-helix structure because of the hydrophobic environment of the cell membrane [28]. The results confirmed that the negative charge of the bacterial envelope contributes to the attraction of the cationic AMP and that the AMP of the helix has an amphiphilic structure (Figure 4). As described above, the pathogenic potential of resistant strains hinders the attachment to surfaces and biofilm formation [29]. We evaluated whether the parent peptide and its analogs inhibit biofilm formation or eliminate biofilm formed by *A. baumannii* and *S. aureus*. We found that analog peptides inhibit and eliminate biofilm formation at concentrations lower than that by Hylin a1 (Figures 5–8). The present findings suggest that the analog peptides Hylin a1-11K and Hylin a1-15K are potential therapeutic agents with superior anti-biofilm activity. When antibiotic peptides are developed, it is necessary to identify instability problems such as degradation by proteases under high-salt concentrations or metabolic processes [30]. Our results confirmed that under high salt concentrations, the analog peptide structures were maintained in human serum. Treatment with rather high salt concentrations confirmed that all peptides in *S. aureus* retained similar activities to the conventional MIC values. However, the MIC values of the parent peptide, Hylin a1-2A, and Hylin a1-3K in divalent ions ($MgCl_2$) showed no activity in *A. baumannii* with increasing salt concentrations. In LPS of Gram-negative bacteria, and divalent ions combined to stabilize and maintain the integrity of the outer membrane [31], the parent peptide, Hylin a1-2A, and Hylin a1-3K showed difficulty in completely killing *A. baumannii*. Therefore, our results suggest that Hylin a1-11K and Hylin a1-15K induce the death of *A. baumannii* without being affected by divalent ions (Table 5). In addition, the greatest weakness of peptide-based drugs is proteolysis by proteases during metabolic degradation [30]. We confirmed that the peptide structures were maintained in human serum (Table 6). Evaluation of the resistant strains showed that the parent peptide, Hylin a1, had a

2–32-fold lower antimicrobial activity compared to the MIC values. However, Hylin a1-11K and Hylin a1-15K showed slightly reduced or similar activity to the MIC values in all strains. LUVs artificially formed mammalian cell membranes and were used to examine AMP-induced calcein leakage (Figure 9). PC: CH (mammalian cell) showed lower calcein release of Hylin a1-11K and Hylin a1-15K than Hylin a1. This suggests that Hylin a1, which hemolyzes RBCs, is toxic, whereas Hylin a1-11K and Hylin a1-15K had much lower toxicity levels. Hylin a1-11K and Hylin a1-15K showed strong release of calcein in liposomes to PE: PG (Figure 10). In a previous study, Hylin a1 was shown to be more effective against Gram-positive bacteria than against Gram-negative bacteria because of the electrostatic potential in the POPE of Gram-negative bacteria [32, 33]. Our results suggests that Hylin a1-11K and Hylin a1-15K have a broad spectrum and induce the death of bacteria when their membrane composition is confirmed. We analyzed the mechanism of action of the four analog peptides compared to that of the parent peptide. AMPs interact with bacterial cell membranes [34]. To analyze the bacterial membrane, NPN was used to measure fluorescence release to the outer membrane. An inner membrane permeability assay was performed using ONPG, cytoplasmic depolarization assay with diSC_3-5, permeation of the cell membrane assay with SYTOX green, and flow cytometry assay with PI. The effect of analog peptides on the bacterial membrane was evaluated. Our results confirmed that analog peptides damage the outer membranes of *A. baumannii* and *S. aureus*, resulting in increased fluorescence. In addition, *E. coli* expressing ONPG increased the intensity through the inner membrane and induced cytoplasmic membrane depolarization by increasing the fluorescence intensity of diCS_3-5. SYTOX green also demonstrated complete membrane disruption as increased fluorescence intensity through binding of Hylin a1 and analog peptides, Fluorescence-activated cell sorting analysis also suggested that the analog peptides completely disrupted the membrane with increasing fluorescence intensity of PI (Figures 11–15). LPS and LTA are formed by Gram-negative bacteria and Gram-positive bacteria and are endotoxins of the bacterial outer membrane. LPS and LTA induce human sepsis shock and immune responses, respectively. We performed CD spectroscopy to confirm the binding affinity of the analog peptides

(Figure 16). While the parent peptide and four analog peptides bound strongly to LTA to confirm the alpha-helix structure, only Hylin a1, Hylin a1-11K, and Hylin a1-15K showed an α-helix structure for LPS. In conclusion, Hylin a1-11K and Hylin a1-15K can interact with endotoxins of all bacteria to inhibit or kill them and are effective against endotoxin-induced inflammation. Infection of bacteria is an essential response in the body. However, persistent inflammatory reactions can lead to diseases such as rheumatism and autoimmune disease. It is important to reduce cytokine expression to prevent continued inflammation. TNF-α, a potent pro-inflammatory cytokine with an important role in the immune system [35], IL-6, and IL-1β are pro-inflammatory cytokines that respond to infections, causing rapid and temporary tissue damage [36, 37]. Hylin a1-11K and Hylin a1-15K showed anti-inflammatory effects in mouse macrophages infected with EJ *A. baumannii* 10 at concentrations of 0.5x and 1x MIC (Figure 17). We will further study the exact mechanism by which the analog peptides triggered an inflammatory response. In conclusion, Hylin a1 analog peptides were synthesized by substitution with lysine and alanine. The analog peptides, Hylin a1-11K and Hylin a1-15K, showed broad-spectrum antimicrobial activity against various strains and MDR strains, and were effective against biofilm formation. At effective concentrations, the analogs did not induce hemolytic activity compared to the parent peptide. The analog peptides have a structure that is stable in physiological environments and active in bacterial-mimic environments, killing bacteria through a mechanism of action that disrupts the bacterial membrane [3]. In addition, anti-inflammatory responses were observed as down-regulated expression of proinflammatory cytokines. The analog peptides Hylin a1-11K and Hylin a1-15K are promising candidates for treating MDR strain infections.

VI. References

1. Pendleton, J.N., S.P. Gorman, and B.F.J.E.r.o.a.-i.t. Gilmore, Clinical relevance of the ESKAPE pathogens. *Expert Rev Anti Infect Ther*, 2013. **11**(3): p. 297-308.
2. Mulani, M.S., et al., Emerging strategies to combat ESKAPE pathogens in the era of antimicrobial resistance: a review. *Front Microbiol*, 2019. **10**.
3. Hsu, L.Y., et al., Carbapenem-resistant Acinetobacter baumannii and Enterobacteriaceae in south and southeast Asia. *Ciln Microbial Rev*, 2017. **30**(1): p. 1-22.
4. Viehman, J.A., M.H. Nguyen, and Y.J.D. Doi, Treatment options for carbapenem-resistant and extensively drug-resistant Acinetobacterbaumannii infections. *Drugs*, 2014. **74**(12): p. 1315-1333.
5. Bahar, A.A. and D.J.P. Ren, Antimicrobial peptides. *Pharmaceuticlas (Basal)*, 2013. **6**(12): p. 1543-1575.
6. Giuliani, A., G. Pirri, and S.J.O.L.S. Nicoletto, Antimicrobial peptides: an overview of a promising class of therapeutics. *Central European Journal of Biology*, 2007. **2**(1): p. 1-33.
7. Haney, E.F. and R.E.J.P.S. Hancock, Peptide design for antimicrobial and immunomodulatory applications. *Biopolymers*, 2013. **100**(6): p. 572-583.
8. Fjell, C.D., et al., Designing antimicrobial peptides: form follows function. *Nat Rev Drug Discov*, 2012. **11**(1): p. 37.
9. Kang, H.K., et al., Antimicrobial and immunomodulatory properties and applications of marine-derived proteins and peptides. *Mar Drugs*, 2019. **17**(6): p. 350.
10. Saint Jean, K.D., et al., Effects of Hydrophobic Amino Acid Substitutions on Antimicrobial Peptide Behavior. *Probiotics Antimicrob Proteins*, 2018. **10**(3): p. 408-

419.

11. Shai, Y.J.B.e.B.A.-B., Mechanism of the binding, insertion and destabilization of phospholipid bilayer membranes by α-helical antimicrobial and cell non-selective membrane-lytic peptides. *Biochim Biophys Acta*, 1999. **1462**(1-2): p. 55-70.
12. Castro, M.S., et al., Hylin a1, the first cytolytic peptide isolated from the arboreal South American frog Hypsiboas albopunctatus ("spotted treefrog"). *Peptides*, 2009. **30**(2): p. 291-296.
13. Fields, G.B., R.L.J.I.j.o.p. NOBLE, and p. research, Solid phase peptide synthesis utilizing 9-fluorenylmethoxycarbonyl amino acids. *Int J Pept Protein Res*, 1990. **35**(3): p. 161-214.
14. Reller, L.B., et al., Antimicrobial susceptibility testing: a review of general principles and contemporary practices. *Clin Infect Dis*, 2009. **49**(11): p. 1749-1755.
15. Mayer, L., M. Hope, and P.J.B.e.B.A.-B. Cullis, Vesicles of variable sizes produced by a rapid extrusion procedure. *Biochim Biophys Acta*, 1986. **858**(1): p. 161-168.
16. Lin, Q. and E.J.P.o. London, Preparation of artificial plasma membrane mimicking vesicles with lipid asymmetry. *PLOS One*, 2014. **9**(1): p. e87903.
17. Loh, B., et al., Use of the fluorescent probe 1-N-phenylnaphthylamine to study the interactions of aminoglycoside antibiotics with the outer membrane of Pseudomonas aeruginosa. *Antimicrob Agents Chemother*, 1984. **26**(4): p. 546-551.
18. Dempsey, C.E.J.B.e.B.A.-R.o.B., The actions of melittin on membranes. *Biochim Biophys Acta*, 1990. **1031**(2): p. 143-161.
19. Feoktistova, M., P. Geserick, and M.J.C.S.H.P. Leverkus, Crystal violet assay for determining viability of cultured cells. *Cold Spring Harb Protoc*, 2016. **2016**(4): p. pdb. prot087379.

20. Erridge, C., et al., Structure and function of lipopolysaccharides. *Microbes Infect*, 2002. **4**(8): p. 837-851.

21. Percy, M.G. and A.J.A.r.o.m. Gründling, Lipoteichoic acid synthesis and function in gram-positive bacteria. *Annu Rev Microbiol*, 2014. **68**: p. 81-100.

22. Dijkshoorn, L., A. Nemec, and H.J.N.r.m. Seifert, An increasing threat in hospitals: multidrug-resistant Acinetobacter baumannii. *Nat Rev Microbiol*, 2007. **5**(12): p. 939.

23. Pea, F., et al., Daptomycin underexposure in a young intravenous drug user who was affected by life-threatening Staphylococcus aureus-complicated skin and soft tissue infection associated with bacteraemia. *Infection*, 2014. **42**(1): p. 207-210.

24. McConnell, M.J., L. Actis, and J.J.F.m.r. Pachón, Acinetobacter baumannii: human infections, factors contributing to pathogenesis and animal models. *FEMS Microbiol Rev*, 2013. **37**(2): p. 130-155.

25. Donlan, R.M.J.E.i.d., Biofilms and device-associated infections. *Emerg Infect Dis*, 2001. **7**(2): p. 277.

26. Spellberg, B., et al., Novel approaches are needed to develop tomorrow's antibacterial therapies. *AM J Pespir Crit Care Med*, 2015. **191**(2): p. 135-140.

27. Jiang, Z., et al., Effects of net charge and the number of positively charged residues on the biological activity of amphipathic α-helical cationic antimicrobial peptides. *Biopolymers*, 2008. **90**(3): p. 369-383.

28. Avitabile, C., L.D. D'andrea, and A.J.S.r. Romanelli, Circular dichroism studies on the interactions of antimicrobial peptides with bacterial cells. *Scientific Reports*, 2014. **4**: p. 4293.

29. Bjarnsholt, T.J.A., The role of bacterial biofilms in chronic infections. *APMIS Suppl*, 2013. **121**: p. 1-58.

30. Powell, M.F., et al., Peptide stability in drug development. II. Effect of single amino acid substitution and glycosylation on peptide reactivity in human serum. *Pharm Res*, 1993. **10**(9): p. 1268-1273.

31. KAMeL ABD ghAni, M.J.S.M., Divalent cations (Mg2+, Ca2+) protect bacterial outer membrane damage by Polymyxin B. *UKM Experts*,2013. **42**(3): p. 301-306.

32. SF Alves, E., et al., Micelle bound structure and model membrane interaction studies of the peptide Hylin a1 from the arboreal South American frog Hypsiboas albopunctatus. *Protein Pept Lett*, 2015. **22**(8): p. 719-726.

33. Epand, R.M. and R.F.J.J.o.P.S. Epand, Bacterial membrane lipids in the action of antimicrobial agents. *Journal of Peptide Science*, 2011. **17**(5): p. 298-305.

34. Lee, J.-K., et al., Antimicrobial HPA3NT3 peptide analogs: placement of aromatic rings and positive charges are key determinants for cell selectivity and mechanism of action. *Biochimica et Biophysica Acta (BBA) – Biomembranes*, 2013. **1828**(2): p. 443-454.

35. Zelová, H. and J.J.I.R. Hošek, TNF-α signalling and inflammation: interactions between old acquaintances. *Inflamm Res*, 2013. **62**(7): p. 641-651.

36. Tanaka, T., M. Narazaki, and T.J.C.S.H.p.i.b. Kishimoto, IL-6 in inflammation, immunity, and disease. *Cold Spring Harb Perspect Biol*, 2014. **6**(10): p. a016295.

37. Ren, K. and R.J.B.r.r. Torres, Role of interleukin-1β during pain and inflammation. *Brain Res Rev*, 2009. **60**(1): p. 57-64.